UNIVERSIDADE D
COIMBRA

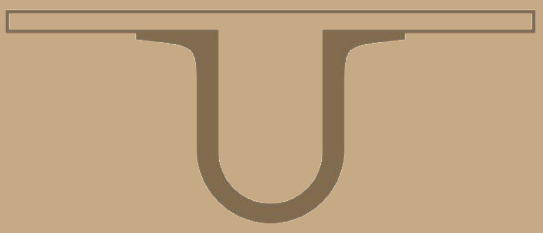

Tiago Miguel Pedro do Couto

HEAT TRANSFER MODELLING IN A COMBUSTION CHAMBER AND SMOKE TUBES OF A BIOMASS BOILER

Master Dissertation in Mechanical Engineering in the speciality of Energy and Environment supervised by Professor José Manuel Baranda Ribeiro, presented to the Department of Mechanical Engineering of the Faculty of Sciences and Technology of the University of Coimbra

February 2019

UNIVERSIDADE D COIMBRA

FACULDADE DE CIÊNCIAS E TECNOLOGIA

Heat Transfer Modelling in a Combustion Chamber and Smoke Tubes of a Biomass Boiler

Submitted in Partial Fulfilment of the Requirements for the Degree of Master in Mechanical Engineering in the speciality of Energy and Environment

Author

Tiago Miguel Pedro do Couto

Advisor

Doctor José Manuel Baranda Moreira da Silva Ribeiro

Jury

President	**Professor Doctor José Carlos Miranda Góis** **Professor at University of Coimbra**
Vowel	**Master João Pedro Pereira** **Auxiliary Researcher at University of Coimbra**
Advisor	**Professor Doctor José Manuel Baranda Ribeiro** **Auxiliary Professor at University of Coimbra**

Coimbra, February 2019

To my invaluable family and friends.

ACKNOWLEDGEMENTS

This dissertation allowed me to better understand the scientific efforts done by people who worked hard through many years to accomplish the knowledge here demonstrated. To them I am extremely grateful, but also there are several people that helped me in a much more direct way and to whose I demonstrate my entire appreciation.

To Dr. José Baranda Ribeiro and Dr. Ricardo Mendes for their support and shared knowledge throughout this entire year, and for the guidance during the completion process of this work. Also, I am very grateful to have had this opportunity to work with Dr. Ribeiro who always given me the confidence I did not have to complete this dissertation.

To João Pedro Pereira for his continuous assistance and helpful advices from the very start of this work, and for the availability and shared valuable experimental data which helped me to improve the results of this work.

To my mother, Ondina Pedro, and father, Luís Couto, a very special thank for their continuous belief and encouragement throughout these six years at university which would have not been possible without their sacrifices and active support when I most needed, and for giving me everything I could ask for to finish this great part of my life.

To my sister, Ana Rita Couto, for accompanying me during this journey, helping me with her company and support. Also, for her availability to aid me when I needed.

Lastly, I want to thank all my fellow friends and family for all the motivation and willingness to help me during this college years. Especially to David, Miguel, Manuel, Ricardo Mendes and Ricardo Santos for their support throughout this student career, for their availability, presence and invaluable friendship.

ABSTRACT

The objective of this dissertation is to develop a heat transfer model for a 3-pass fire-tube 578 kW boiler using biomass as fuel. To fully characterize this biomass boiler, a numerical program was created in MATLAB where several thermodynamic correlations were needed to develop a combustion model which predicts several important output parameters such as the adiabatic flame temperature and the flue gases mass flow rate that will be used in the following model.

The heat transfer model predicts the boiler's total energy transferred from flue gases to the surrounding surfaces. An energy balance was established in each boiler section to evaluate the amount of energy generated by the combustion gases and the amount of heat transferred to the inner walls of the system.

It was also studied and further explained the influence of radiation in the furnace zone (1st boiler pass), and the extreme importance of the flue gases high temperatures which promote large amount of radiative values. In the convection sections which includes the smoke tubes, the convective heat is much more prominent due to the lower flue gas temperatures.

Then, to validate this custom model, simulated results were evaluated, such as furnace and chimney outlet temperatures, as well as, the boiler's thermal output power which values were then compared to experimental data gathered from six different output power boilers in steady-state conditions. Finally, the model results showed good agreement with all the six boiler tests.

Keywords Smoke-Tube Boiler, Biomass, Combustion, Heat Transfer, Thermal Power.

RESUMO

O objetivo desta dissertação resume se ao desenvolvimento de um modelo de transferência de calor para uma caldeira de tubos de fumo de 3 passes a biomassa com uma potência térmica de 578 kW. Para modelar numericamente o processo intrínseco à caldeira, recorreu se ao MATLAB onde se considerou várias correlações necessárias ao desenvolvimento de um modelo de combustão. Este modelo determina vários parâmetros de saída, como a temperatura adiabática de chama e o caudal mássico de gases, que serão essenciais para a criação do modelo seguinte.

O modelo de transferência de calor prevê a energia total transferida dos gases de combustão para as superfícies internas da caldeira. Um balanço energético foi estabelecido em cada secção principal da caldeira para avaliar a energia gerada pelos gases de combustão e a quantidade que é efetivamente libertada para as paredes circundantes do sistema.

Explicou se o efeito e influência da radiação na zona da fornalha e a grande importância que as temperaturas altas têm ao promover enormes quantidades de calor radiativo. Nas zonas de convecção que incluem os tubos de fumo, o calor transferido por convecção é muito mais relevante pelas menores temperaturas dos gases de combustão.

Posteriormente, para validar o modelo criado, foram avaliados os resultados da simulação tais como as temperaturas de saída da fornalha e da chaminé, e ainda a potência térmica da caldeira. Estes valores foram seguidamente comparados com valores experimentais obtidos através de seis caldeiras com potências térmicas diferente em condições estacionárias. Por fim, os resultados do modelo demonstraram estar de acordo com todos os testes feitos às seis caldeiras.

Palavras-chave: Caldeira de Tubos de Fumo, Biomassa, Combustão, Transferência de Calor, Potência Térmica.

CONTENTS

LIST OF FIGURES

SYMBOLOGY AND ACRONYMS

Symbology

1 – 1st Boiler pass (Radiation section i.e., Furnace)

2 – 2nd Boiler pass (1st Convection section)

3 – 3rd Boiler pass (2nd Convection section)

α- Absorptivity

ε– Emissivity

ε_r – Rugosity friction

λ_{st} – Theoretical air coefficient

λ_{real} – Air coefficient in real conditions

μ – Dynamic viscosity $[kPa\ s]$

χ – Additional fuel fraction in the reactants side

ρ – Specific mass $[kg/m^3]$

A_i – Total area of each boiler section $[m^2]$

AF – Air-Fuel ratio

amb – Ambient state

bio – Relative to dry biomass

$cond$ – Conduction

$conv$ – Convection

C_p – Heat capacity at constant pressure $[kJ/kmol\ K]$

d – Oxygen quantity in products [%]

D – Diameter $[m]$

$exit$ – Boiler chimney

ext - External

eq - Equivalent

fg – Flue gases

f – Mass fraction

fur – Furnace

H – Enthalpy $[kJ/kmol_{bio}]$

HV – Heat value $[kJ/kg\ K]$

h –Heat transfer coefficient $[W/m^2\ K]$

i – Notation representing each slice

in – inlet of a section

int – Internal section

j – Notation representing a chemical substance or element

K – Corrective factor

k – Thermal conductivity $[W/m\ K]$

L_i – Length or Height of each boiler section

liq – Liquid state

M_i – Molar mass of i element $[kg/kmol]$

m – Related to a mean thickness of a section

$\dot{m}$ – Mass flow $[kg/s]$

n – Notation representing each boiler section (1,2,3)

n_j – Number of moles of each product substance

$N_{i,slices}$ – Number of i slices

N_j – Number of j product substances

N_{tubes} – Number of tubes

Nu – Nusselt number

out – Outlet of a section

p_{amb} – Ambient pressure $[kPa]$

P_{therm} – Boiler output power $[kW]$

Pr – Prandtl number

Q – Heat transfer $[kJ/kmol_{bio}]$

$\dot{Q}$ – Heat transfer rate $[kJ/s]$ or $[kW]$

rad – Radiation

ref – Reference state

Re – Reynolds number

T – Temperature $[K]$

$\bar{T}$ – Average temperature

T_{flame} – Adiabatic flame temperature $[K]$

$wall$ – Wall (heat transmitting surface)

Acronyms

DHW – Domestic Hot Water

EU – European Union

ORC – Organic Rankine Cycle

DEM – Department of Mechanical Engineering

FCTUC – Faculty of Sciences and Technology of the University of Coimbra

LHV – Lower Heat Value

UC – University of Coimbra

1. INTRODUCTION

1.1. Motivation and Objectives

As world population keeps growing, the energy to sustain people's necessities is increasing at an alarming rate. The dependency on energy is directly correlated to the high usage of electronic products and comfort demand, which became fundamental on our lives over the last decades.

From the beginning of the XX century the planet has been increasingly affected by greenhouse gases following the arise of industrial revolution. In recent studies, the emission of polluted gases from fossil fuels have been proved to be one of the major causes of the global warming.

As climate changes are more pronounced nowadays, huge wildfires and abnormal floods have gradually whipped out the planet earth in recent years, many specialists appointed these environmental disasters as a consequence of the high consumerism of fossil fuels (coal, natural gas and oil), widely used in both industrial and domestic sector.

For these reasons, there are alternative energy sources that could support the high demand in a less impactful way such as the use of renewable energy like hydropower, wind, geothermal, solar or biomass.

Aiming to preserve the planet environment while meeting environmental legislations to avoid fines and fossil fuels dependency, many of the industries from various sectors e.g., automotive, agricultural, construction and others, are already investing in renewable energy at an unprecedent rate [1] [2] [3] [4].

Portugal is currently the 7th largest country in EU at producing renewable energy. On March of 2018 [5], the production of renewable energy surpassed the amount of energy consumed, becoming self-governed and non-dependent on fossil fuel energy. This is a clear sign that efforts in clean energy have been made within the scope of a greener country [6].

Until a few years ago, the use of biomass boilers was mainly used by large industries [7] to produce substantial amounts of thermal energy and when integrated in a cogeneration system [8], they could also produce electrical energy to suppress their needs. Nowadays, the biomass boiler market has verified changes in user's paradigm, as there is an increasing demand [9] for this type of boilers to suppress thermal requirements for commercial buildings and domestic services [10] [11], proving that there is a market to explore, forcing new developments on boiler designs with the aim to be more user-friendly.

In order to fulfill the user's needs, the upcoming boilers must be automated to facilitate the equipment's operability in the user's perspective. An automated boiler with both automatic ignition and cleaning features are essential to provide an accessible experience, as well as, the inclusion of an automated excess air controller to provide better combustion efficiency with ease of use.

Following the increase demand of this type of domestic fire-tube boilers, this work tends to explore and study this type of boilers which, until recent years, have not been analysed with much in-depth.

In this dissertation a heat transfer model is suggested and is adapted from smoke-tube boiler studies to analyse and estimate respectively, the heat transfer behaviour and the thermal power of a biomass boiler. Regarding input data, it was necessary to produce a combustion model to gather initial values that will be assigned to the development of a heat transfer model. This work will then be validated with experimental results.

This work may be a useful tool for upcoming innovative designs of fire-tube boilers using pellets as fuel. It will also be suitable as an informative support for boiler projects in Energy Project subject, providing helpful insights to students.

1.2. Structure of Dissertation

Chapter 2 refers to the boiler configuration and its operation. The major boiler components are described, while its functions are explained as its importance on the combustion and heat transfer models. It is also clarified the flue gases behavior throughout the boiler from its ignition to their exhaust.

Chapter 3 explains the purpose of creating a combustion model for the studied boiler. Four different situations are studied between theoretical and real conditions to understand how moisture can influence various output parameters of combustion model. Additionally, the adiabatic flame temperature and mass-flow rate were the main parameters determined which will be useful on the upcoming heat transfer model.

Chapter 4 shows the theoretical support of a heat transfer modelling, using as reference five analogous studies of fire-tube boilers based on thermodynamic principles and correlations where both similarities and differences of each study approach are explained. It also suggests a custom heat transfer model applied to this case, heavily based on the case studies and on the "Fundamentals of Heat and Mass Transfer" book wrote by Incropera et al.

Chapter 5 demonstrates simulated data from the heat transfer model. Various graphics and figures are displayed, showing comparisons between the model's output data and the experimental values. These comparisons were done in order to provide some additional explanations on the differences between the obtained values.

Chapter 6 provides an overall discussion on the approached combustion and heat transfer models for the studied 3-pass smoke-tube boiler, as well as, evaluating upcoming perspectives to further improve this study.

2. BOILER CONFIGURATION

2.1. Peripherals

2.1.1. Hopper

The hopper is an enclosed silo with pyramidal shape that stores biomass and allows it to be fed through gravity to a worm-screw. Most hoppers are made from metal or plastic, allowing low cost maintenances. It is a reservoir that feeds solid fuels and preserves its properties. In this case, pellets are used as fuel, they have some advantages over wood and other types of unprocessed biomass, such as higher energy density, homogeneous heat content and particle size, and although it is more expensive, this type of pellets provide better combustion efficiency. As pellets are condensed, the storage requirements are small, helping to cut down costs.

The installed feeder in Figure 2.1 has a capacity of 500 dm^3 and operates by an electric motor that can be programmed to dispense an exact amount of biomass desired. These systems are the most cost effective when installed in narrow places, being particularly efficient when transporting pellets on a limited area.

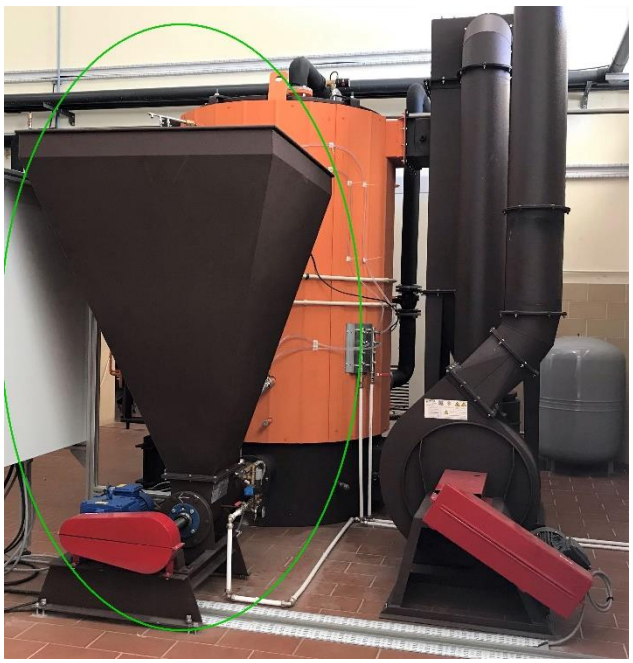

Figure 2.1. (a) Hopper (green circle) installed on the boiler system.

2.1.2. Worm-screw Supplier

The worm screw allows to transfer the solid fuel from the hopper into the combustion chamber. The amount of biomass fed into the combustion chamber at each moment depends on the power demand. This equipment has an electric motor with controllable speed to increase or decrease the fuel flow rate.

Figure 2.2. (a) Biomass carried by worm-screw **(b)** Worm-screw and structure.

2.1.3. Combustion Chamber

The most important zone of the studied boiler is the combustion chamber (i.e., furnace) where most of the energy produced is transferred to the surrounding walls.

The studied chamber has a cylindrical shape and has two distinct sectors. The lower sector, showed in Figures 2.3 (a) and (b), is where the fuel and air join altogether causing the combustion. This chamber's zone has an isolated ceramic concrete to avoid material erosion and is considered that no energy is transferred to the surroundings. Also, this section, also called the burner zone, is where the fire ignition of the mixture starts. During this combustion process, very high temperatures are produced by the flame, which are transmitted to surrounding walls and to the bottom of the fuel. The air introduced in this sector also contributes to a greater heat flux transferred to the surface, degrading the biomass at a higher rate.

Due to the high temperatures, the pyrolysis effect starts, changing the compositions of chemical burned gases that occurred in the beginning of the combustion process. This combustion process behaviour and the production of flue gases products are

very complex to convert into numerically equations due to several factors (later explained), that promote a faster biomass degradation.

Figure 2.3. (a) CAD model of the chamber's lower section **(b)** Furnace door where biomass is transferred.

As seen in the following schematic representation, heat and mass transfer processes are produced in the lower section of the combustion chamber where the flame's heat flux as well as heat losses irradiate the chamber's surface base [12].

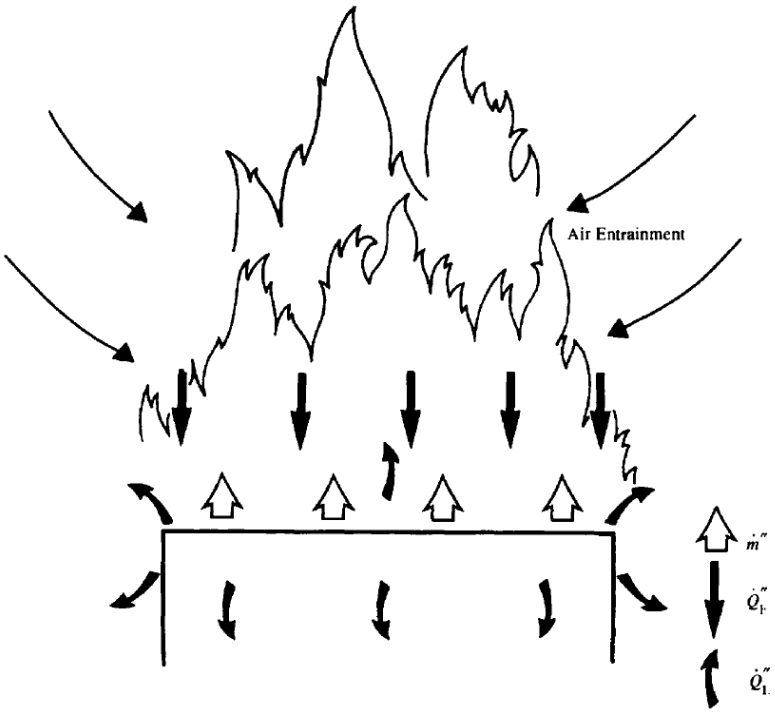

Figure 2.4. Representation scheme of a burning surface (Furnace lower section) showing a heat fluxes in with highly non-linear behaviour from the surface $\dot{m}$", flame heat $\dot{Q}_F$" to the surface and losses $\dot{Q}_l$" [12].

Furnace's higher sector is where the heat of combustion products will be transferred to the surrounding surfaces assuming an isobaric process. The walls are made from the same material as the smoke tubes and its area is large enough to dissipate the most energy produced [13]. The following heat transfer model presented in chapter 4, will take into account only the higher sector of the furnace in which, the adiabatic temperature flame value is calculated from this sector's base surface.

2.1.4. Vertical Smoke-Tubes

The smoke tubes are mounted vertically and separated from each other by equal distances. There are two passes of smoke-tubes in the studied boiler. A "first pass tubes" is defined by a group of 22 tubes, while the "second pass" has 20 tubes, both having the same dimensions and thermal properties. Objectively, flue gases pass through the inside of these tubes at high temperatures, transferring the thermal energy to the surrounding water. The tubes' internal surfaces are prone to dirtiness by the gas flow, adding thermal resistance to the heat surface transfer. Hence, cleaning the internal surfaces of tubes are ultimately important to not only reduce the friction between the hot gases and the tube's internal surfaces but also to obtain the maximum power efficiency transferred.

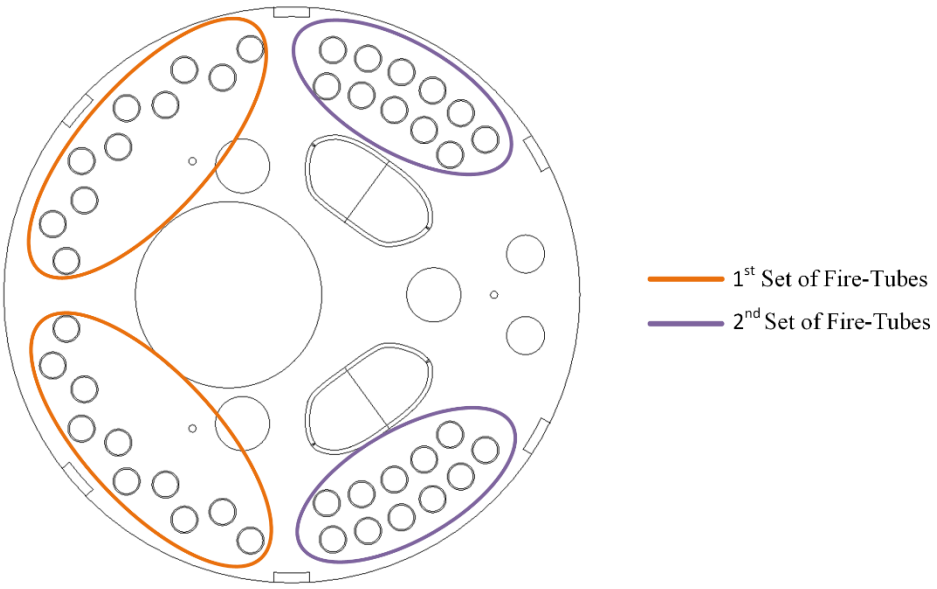

Figure 2.5. Boiler top view highlighting the two passes of smoke-tubes.

2.1.5. Induced Draft and Forced Draft Fans

To ensure a complete combustion of the biomass transferred into the combustion chamber, it is necessary to guarantee that enough oxygen is introduced in the chamber. To this end, forced draft fans are installed on the bottom of the boiler, sending the necessary amount of ambient air to the biomass combustion. The induced draft fans are installed at the outlet of the multicyclone filter system to extract cleaned flue gases from the boiler by generating depression within the furnace. The induced fans are exposed to elevated temperatures and are prone to corrosion. Both fans can be controlled to adjust the (de)pressure in the combustion and the oxygen content in the airflow rate.

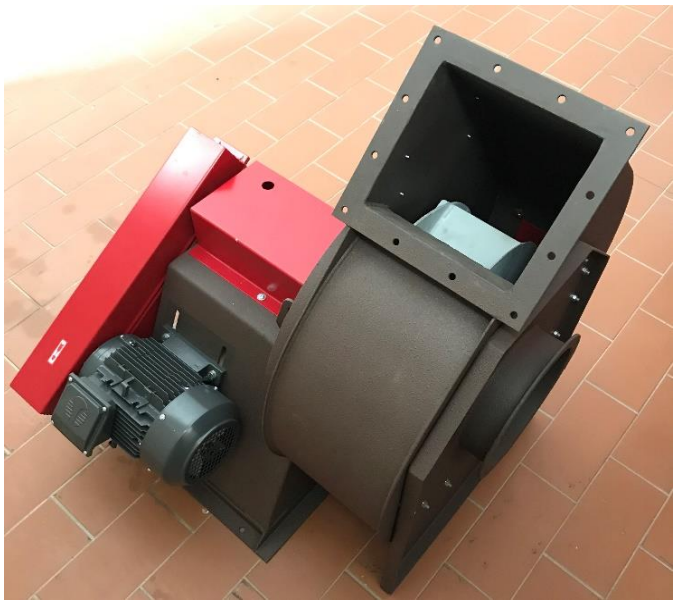

Figure 2.6. Induced draft fan for the boiler system.

2.1.6. Cyclone Separation System

This boiler has also a pyramidal/rectangular shaped cyclone system (Figure 2.7) installed between the boiler and the induced draft fan, which purpose is to extract the solid particles (e.g. volatile ashes and soot) present on the flue gases from the combustion of the biomass. The uncleaned flue gases enter through the side of the filtration system, moving down along the walls by a descendent vortex, passing then, through a conical shaped section where the flue gases invert their direction by an ascendant vortex. Later, the now cleaned flue gases are exhausted from the top of the separation cyclone whereas the solid dirt is retained in a reservoir installed on the bottom of the system.

Figure 2.7. Multiple cyclone system (red circle) installed on the boiler system.

2.2. Principles of Boiler Operation

Fire-tube boilers can reach high efficiency levels [13] due to its well-made design that absorbs the flue gases heat throughout its entire gas route. The wall surfaces have great thermal conductibility and major energy losses are due to the non-exploited flue gases temperatures that exit the boiler chimney.

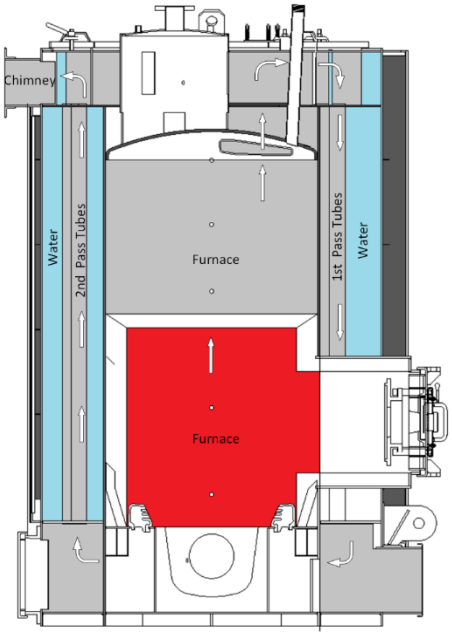

Figure 2.8. Flue gases path represented on boiler schematic. drawing.

The flue gases path is exemplified by the arrows in Figure 2.8. The hot gases produced from combustion start at the beginning of the furnace's higher section, ascending then, to the first inversion box, while transferring most of its internal energy to the side surfaces. Then, the hot gases descend through the first pass tubes until they reach the half of the second inversion box, transferring also thermal power to the surrounding surfaces. After, the flue gases go to the 2nd pass of tubes while transferring much less thermal energy than the previous sectors. At last, they ascend to the chimney (i.e., 3rd inversion box), where the gas will be exhausted to a multiple cyclone system that aims to reduce flue gases emission particles sent to the atmosphere.

3. COMBUSTION ANALYSIS

A combustion process is defined as the production of both heat and light through an exothermic chemical reaction between a fuel and an oxidizer (usually atmospheric air). This process generates gaseous products at very high temperatures containing a large amount of energy.

Most solid fuels have in their composition C, H, O, S and N molecules, while atmospheric air has generally O_2 and N_2. Shortly after starting the combustion process, the chemical products such as CO_2 and H_2O are formed inside the studied furnace. Nonetheless, the presence of ashes will not be considered on this model for simplified calculations purposes and since the latter results would not change considerably. The type of biomass used in this work was pellets from red pine. This selected type biomass is composed by four chemical species: carbon, oxygen, hydrogen and nitrogen.

The mass fraction (%) of such chemical species in dry biomass are shown on the graphic of the Figure 3.1.

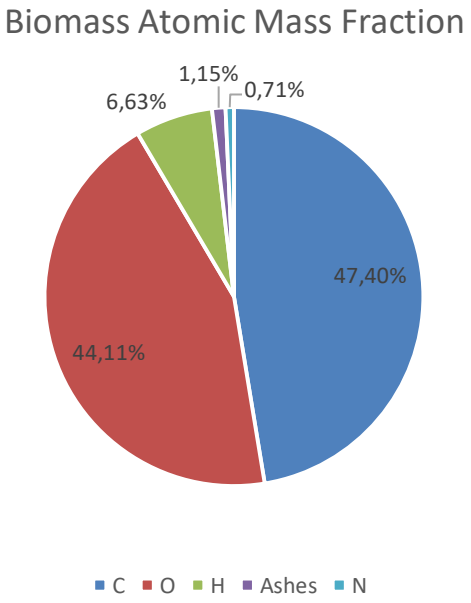

Figure 3.1. Mass fraction of each biomass chemical substances.

Later, the biomass mass fractions were converted into molar fractions by dividing the mass fractions with the molar mass of each chemical specie. This conversion eases the upcoming chemical balances, allowing better cohesiveness between MATLAB's calculations and Refprop's data units. The following calculations throughout this chapter were based on equations from [14]. The Refprop software was used in this work as a fluid database from which several fluid properties can be evaluated for different states using MATLAB.

The chemical formula corresponding to 1 kmol of dry biomass is depleted by:

$$C_{0,0395}\ H_{0,0628}\ N_{0,00051} O_{0,0276} \tag{3.1}$$

The fuel's HV is the amount of heat that can be exploited from a complete combustion process in which the reactants and the combustion products are at the reference conditions. The biomass HV is also known as the absolute value of the fuel's enthalpy of combustion.

$$HV = LHV = |H_{comb}| \tag{3.2}$$

Only the biomass LHV was considered since the water existing in the combustion products is in the vapor form and never condensed.

3.1. Requirements

To initiate the combustion model, data inputs are required. The main purpose of MATLAB's calculations is to determine the quantity of combustion products, the adiabatic flame temperature and the flue gases mass flow at the following initial conditions:

- Pressure in the furnace → $P_{fur} = 101{,}325\ kPa$
- Combustion air temperature → $T_{amb} = 290.15\ K$
- Reference temperature → $T_{ref} = 298.15\ K$
- Combustion air relative humidity → $h_{amb} = 70\%$

- Boiler nominal output → $P_{ther} = 578\ kW$
- Biomass heat value → $LHV = 18{,}92\ kJ/kg$
- Moisture in biomass → $h_{bio} = 10\%$
- Quantity of oxygen in products → $d = 6{,}5\%$

Some of the above-mentioned conditions such as the P_{fur}, T_{amb} and h_{amb} correspond to the average values experimentally determined. The reference temperature T_{ref} is considered a constant value. It was also assumed that the biomass temperature is the same as the reference temperature while the maximum boiler thermal power (P_{ther}) was supplied by manufacturer Ventil [13].

3.2. Combustion Reactions

Four types of combustion conditions were subject of in-depth analysis:

- Theoretical reaction with dry biomass.
- Theoretical reaction with moisture in biomass.
- Real reaction with excess air and with dry biomass.
- Real reaction with excess air and moisture in biomass and combustion air.

3.2.1. Theoretical Reaction with Dry Biomass

$$C_{0,0395}\ H_{0,0628}\ N_{0,00051} O_{0,0276} + \lambda_{st}(O_2 + 3{,}76N_2) \rightarrow aCO_2 + bH_2O + cN_2 + dO_2 \quad (3.3)$$

The terms in the parentheses represent the dry air composition which contains 1 kmol of O_2. In this situation, the quantity of O_2 in the products equals to zero since the aim of this chemical equation is to determine the minimum quantity of dry air needed to fulfill a complete combustion, i.e., where all oxygen is consumed ($d = 0$).

$$\begin{cases} n_C \rightarrow 0{,}0395 = a \\ n_H \rightarrow 0{,}0628 = 2b \\ n_N \rightarrow\ 0{,}00051 + 7{,}52\lambda_{st} = 2c \\ n_O \rightarrow 0{,}0276 + \lambda_{st} = 2a + b + 2d \end{cases} \tag{3.4}$$

The unknown variables (a, b, c) represent the unknown mole numbers of each chemical compound present on the products side. The variables in both sides were calculated and resulted in the following values:

$$\begin{cases} a = 0{,}0395 \\ b = 0{,}0329 \\ \lambda_{st} = 0{,}0421 \\ c = 0{,}1586 \end{cases} [kmol] \tag{3.5}$$

The λ_{st} is defined as the stoichiometric air coefficient, i.e., 1/4,76 of the theoretical number of dry air molecules needed on an ideal combustion situation. The quantity of dry air necessary for this theoretical reaction is $\lambda_{st} = 4{,}76\ x\ 0{,}0421$ kmol per kg of biomass, as defined before, burned.

3.2.2. Theoretical Reaction with moisture in Biomass

$$C_{0,0395}\ H_{0,0628}\, N_{0,00051} O_{0,0276} + n_{H_2O_{bio}} + \lambda_{st}(O_2 + 3{,}76N_2) \rightarrow aCO_2 + bH_2O + cN_2 + dO_2 \tag{3.6}$$

In this part, the molar fraction of the moisture (liquid state) present in dry biomass was assessed. As the chemical balance is based in 1 kmol of dry biomass, the equation 3.4 converts the mass fraction of the biomass moisture into molar fraction.

$$n_{H_2O_{bio}} = \frac{0{,}1}{M_{H_2O}} \tag{3.7}$$

As seen in equation 3.5, the fraction of H_2O in the products increases from the former theoretical reactions, as a result of the considered moisture present in the fuel. Also, the fact that this moisture is in liquid state, does not change the amount of λ_{st} since the

H_2O_{bio} molecules will be directly transformed into H_2O on the products side. Hence, solely the O_2 amount is increased compared to the previous theoretical reactions.

$$\begin{cases} a = 0{,}0395 \\ b = 0{,}0384 \\ \lambda_{st} = 0{,}0421 \\ c = 0{,}1586 \end{cases} [kmol] \tag{3.8}$$

3.2.3. Real Reaction with Excess Air considering moisture in Biomass

In a real condition, yet neglecting ambient air humidity in a first approach, the O_2 fraction in the products side was set at 6.5% (d=0,065) as a first desired input. The analysis of this reaction allowed to highlight the higher air fraction in the reactants compared to the fraction in the theoretical reaction. The presence of oxygen fraction in the products is justified by the increased dry air value on the reactants side.

$$\chi(C_{0{,}0395}\ H_{0{,}0628}\ N_{0{,}00051} O_{0{,}0276} + 0.1\ H_2O_{bio}) + \lambda_{real}\ (O_2 + 3{,}76N_2) \rightarrow aCO_2 + bH_2O + cN_2 + 0{,}065\ O_2 \tag{3.9}$$

To determine the excess air from the data of the gas's analysis and assuming the generated flue gases were completely dried, the following auxiliary expression can be admitted in order to calculate the chemical balances:

$$c = 1 - (a + d) \tag{3.10}$$

From the former balance equation 3.6 and with the auxiliary expressions 3.7 and 3.10, the following equation can be expressed by:

$$\begin{cases} n_C \rightarrow\ 0{,}0395\chi = a \\ n_H \rightarrow\ (0{,}0628 + 0{,}2)\chi = 2b \\ n_N \rightarrow\ 0{,}00051\chi + 7{,}52\lambda_{real} = 2c \\ n_O \rightarrow\ (0{,}0276 + 0{,}1)\chi + 2\lambda_{real} = 2d \end{cases} \tag{3.11}$$

The λ_{real} is useful to evaluate the amount of excess air o burn all the available fuel present in the chamber, while considering moisture in the biomass. The amount of each combustion product is:

$$\begin{cases} n_{CO_2} = 0{,}0395 \\ n_{H_2O} = 0{,}0384 \\ n_{N_2} = 0{,}2287 \\ n_{O_2} = 0{,}0186 \end{cases} [kmol] \tag{3.12}$$

3.2.4. Real Reaction with Excess Air considering Moisture in Biomass and Ambient Air

$$\begin{aligned} (C_{0,0395}\ H_{0,0628}\, N_{0,00051} O_{0,0276} + n\, H_2O_{bio}) + e\, H_2O_{air} \\ + \lambda_{real}(O_2 + 3{,}76N_2) \\ \rightarrow a_{real}\, CO_2 + b_{real}\, H_2O + c_{real}\, N_2 + d_{real}\, O_2 \end{aligned} \tag{3.13}$$

In reality, the combustion process is never completed, although, the chemical balance above (3.13) tries to accurately represent a realistic combustion reaction in the boiler's furnace. Besides the already mentioned simplifications explained through this chapter, its values will not diverge significantly from the experimental results. The values from this reaction will be used as reference for both combustion model's output data and the upcoming heat transfer model. This chemical balance (also shown in Annex A in greater detail) allowed to determine the air coefficient and the molar fractions of each substance on the products side.

$$\begin{cases} n_C \rightarrow\ 0{,}0395\chi = a \\ n_H \rightarrow\ (0{,}0628 + 2n)\chi + 2e = 2b \\ n_N \rightarrow\ 0{,}00051\chi + 7{,}52\lambda_{real} = 2c \\ n_O \rightarrow\ (0{,}0276 + n)\chi + 2e + 2\lambda_{real} = 2d \end{cases} \tag{3.14}$$

Molar fractions for 1 kmol of dry biomass on the products side:

$$\begin{cases} n_{CO_2} = 0{,}0395 \\ n_{H_2O} = 0{,}0423 \\ n_{N_2} = 0{,}2287 \\ n_{O_2} = 0{,}0186 \end{cases} [kmol] \tag{3.15}$$

3.3. Enthalpy of reaction

To evaluate the amount of absorbed or released energy during the combustion process from the chemical balance showed in chapter 3.2.4. and based on [14], it is necessary to calculate the enthalpy of both reactants and products, by the following equation:

$$Enthalpy = \bar{h}_f + \left(\bar{h} - \bar{h}^o\right) \tag{3.16}$$

As seen from the equation 3.11 the total enthalpy equals to the enthalpy of formation since it is admitted that the sensible enthalpy both at a specific state $\left(\bar{h}\right)$ and at reference state $(\bar{h}^o)$ hold the same value. As potential and kinetic energies are also despised, the energy balance relation that translates the steady-flow chemical reaction can be expressed by:

$$E_{in} = E_{out} \tag{3.17}$$

Which can be developed in the alternative balance equation shown below:

$$\begin{aligned} Q_{in} + W_{in} + \sum N_{reac} \left(\bar{h}_f + \bar{h} - \bar{h}^o\right)_{reac} = Q_{out} + W_{out} \\ + \sum N_{prod} \left(\bar{h}_f + \bar{h} - \bar{h}^o\right)_{prod} \end{aligned} \tag{3.18}$$

N_{reac} and N_{prod} are the number of moles of the reactants and products, respectively, per moles of biomass. The sum of the third member in both sides (reactants and products) are respectively, H_{reac} and H_{prod}.

To calculate the flue gases total internal energy, it was previously determined the energy present in both reactants and products. The enthalpy of formation on the products side were obtained from [24].

Biomass' Enthalpy of formation is established by:

$$\bar{h}_{f_{bio}} = LHV + \left(N_{CO_2}\, h_{f_{CO2}} + N_{H_2O}\, h_{f_{H_2O}}\right) \tag{3.19}$$

Reactants and products enthalpies values were obtained respectively by the following equations:

$$\begin{aligned} H_{reac} = \bar{h}_{f_{bio}} + n_{H_2O}\, \bar{h}_{f_{H_2O_{liq}}} + m_{H_2O}\, \bar{h}_{f_{H_2O}} + \lambda \left(\bar{h}_{T_{amb_{O_2}}} - \bar{h}_{T_{ref_{O_2}}}\right) \\ + \; 3{,}76\, \lambda_{real} \left(\bar{h}_{T_{amb_{N_2}}} - \bar{h}_{T_{ref_{N_2}}}\right) \end{aligned} \tag{3.20}$$

$$\begin{aligned} H_{prod} = \left(N\, \bar{h}_f\right)_{CO_2} + \left(N\, \bar{h}_f\right)_{H_2O} + \left(N\left(\bar{h}_{flame} - \bar{h}_{ref}\right)\right)_{CO_2} \\ + \left(N\left(\bar{h}_{flame} - \bar{h}_{ref}\right)\right)_{H_2O} + \left(N\left(\bar{h}_{flame} - \bar{h}_{ref}\right)\right)_{N_2} \\ + \left(N\left(\bar{h}_{flame} - \bar{h}_{ref}\right)\right)_{O_2} \end{aligned} \tag{3.21}$$

Where the products enthalpy from the chemical balance equals to the adiabatic flame enthalpy, as:

$$H_{prod} = H_{flame} \tag{3.22}$$

The energy of the products is then calculated from the already known molar fractions and enthalpies of formation (chemical energy), as well as thermal and physic enthalpies (latent and sensible energies). In a first approach, the exit temperature value is figured out experimentally since there is no other experimental alternative to obtain its value.

During combustion with a steady-flow rate, it is considered that no work is involved throughout the whole combustion process, hence, it is possible to assume the following equation:

$$W_{in} = W_{out} = 0 \tag{3.23}$$

The combustion on the furnace only produces heat output, thus, $Q_{in} = 0$. The total energy generated in the combustion chamber, also known as the enthalpy of reaction, is the heat released through an exothermic chemical reaction which is calculated by:

$$Q_{out} = H_{reac} - H_{prod} \tag{3.24}$$

The total energy produced in the furnace for the studied condition mentioned in chapter 3.2.4, is $Q_{out} = 16101\ kJ/kmol_{bio}$.

3.4. Output Parameters

The output parameters determined by the combustion model are described in the following sub-chapters. These can be useful to better understand and control the combustion performance but also gives insightful data values, such as the adiabatic flame temperature or flue gases flow, which will be needed onto the following heat transfer model.

3.4.1. Excess Air

During a combustion process it is necessary to ensure that all fuel introduced into the chamber is burned. Excess air λ is an informative and important parameter that indicates the additional amount of air needed for a complete burning. It is also characterized as the supplementary fraction of air in the reactants beyond the needed for the theoretical combustion.

On fire-tube boilers is usual to use excess air as an operating control parameter to control the airflow during the combustion process. The air flow adapts to the fuel flow ensuring a minimum amount of excess air to the combustion. Due to the difficulty of directly measuring the air flow rate that enters in the combustion chamber, the air excess is evaluated by defining the quantity of O_2 present in the products, which can also be evaluated by a gas

analyzer. The excess air is then calculated by the ratio between the air coefficients λ_{real} and λ_{st}, existing in the reactants. As seen in the Figure 3.2, increasing the excess air into the combustion chamber, the quantity of O_2 will rise exponentially.

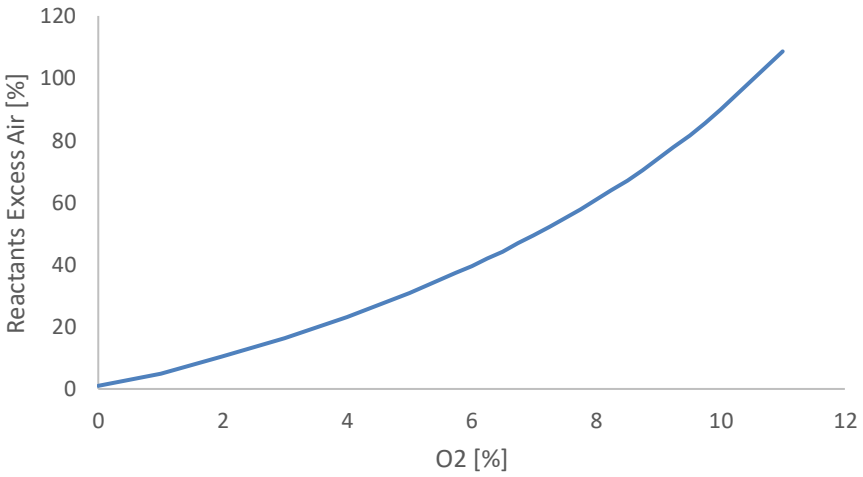

Figure 3.2. Resultant amount of O_2 by increasing the excess air.

The excess air value for this studied case while using the former input data, is:

$$Exc = \frac{\lambda_{real}}{\lambda_{st}} = 1{,}443 \tag{3.25}$$

Which stands for 44,3% of added O_2 than the ideal amount for a complete theoretical combustion.

3.4.2. Air-Fuel Ratio

The Air-Fuel ratio is a fractional parameter used to estimate the mass of air required for a complete combustion when a certain quantity of fuel is used. In a real environment, the amount of air needed to burn the whole present fuel is much higher than theoretical conditions due to the existing moisture in both ambient air and fuel, increasing the difficulty of the combustion process by the extra work needed to vaporize that moisture.

The AF ratio expression admitting the initial inputs is:

$$AF = \frac{\dot{m}_{air}}{\dot{m}_{fuel}} = 8{,}478 \tag{3.26}$$

Knowing the flue gases mass flow rate and the AF value from the combustion model it is possible to verify the flow rate of air or fuel to be used in a steady-flow combustion.

3.4.3. Adiabatic Flame Temperature

The adiabatic flame temperature is the result of a "theoretical" complete combustion without any heat transfer to the surroundings and no realization of work or changes in potential and kinetic energies where it was also assumed a constant atmospheric pressure during the combustion process.

On the combustion chamber, the initial conditions were set at 290.15 K and 70% for the ambient temperature and the air moisture, respectively.

To evaluate the adiabatic flame temperature, it was also necessary to previously estimate the flame energy products, which are already known by the expression 3.20 and flame enthalpy, which equations are showed in Annex A.

The flame temperature was then determined by a "while" cycle where an admissible error between the balance of both reactants and flame enthalpies, was introduced to force the loop to stop when this difference amid the two equations was less than 50 kJ, as shown in Annex A.

$$Error = abs\left(H_{reac} - H_{flame}\right) < 50\ [kJ/kmol_{bio}] \tag{3.27}$$

The adiabatic flame temperature for the assumed initial conditions is:

$$T_{flame} = 1831{,}1\ K \tag{3.28}$$

3.4.4. Flue Gases Rate

The mass flow rate value depends on the boiler output power the sum of all products molar fractions, introduced air-flow rate and the reactants and products enthalpies. During combustion, the gas mass flow rate is considered constant throughout the whole boiler and was based from the real reaction (3.2.4). Its value can be calculated by the further expression:

$$\dot{m}_{fg} = \frac{P_{ther}}{Q_{out}} \left(f_{CO_2,real} + f_{H_2O,real} + f_{N_2,real} + f_{O_2,real}\right) \quad (3.29)$$

Where $f_{j,real}$ refers to the mass fractions of each chemical compound of the products side which are calculated by both molar masses and number moles of each flue gases substance present in the products:

$$f_{j,real} = \left(M_j\ N_j\right)_{real} \quad (3.30)$$

Considering the initial input data values, the flue gases mass flow rate is:

$$\dot{m}_{fg} = 0{,}342\ kg/s \quad (3.31)$$

4. HEAT TRANSFER MODELLING

4.1. Heat Transfer Model

There have been few studies exhibiting comprehensive heat transfer models for smoke-tube boilers. In addition, not even one study on boilers using biomass as fuel was found through Elsevier publisher. Thus, a custom heat transfer model was developed for this work based on various 3 pass fire-tube boiler studies. The burning of biomass produces high temperature flue gases throughout the boiler containing also ashes and soot that will be despised in this work for simplification measurements. Besides that, the following used correlations and equations were used as references to comprehensively explain the boiler's heat transfer model, which is supported by several case studies [13] [15-17]. Although, different types of fuels are used by other studies, the heat transfer equations presented are the same, so it eases the whole calculation process. First, it is necessary to define the input data related to the boiler's initial conditions.

This model requires the following data inputs:

- Flue gases mass flow
- Boiler geometry
- Adiabatic flame temperature
- Wall surfaces properties
- Wall average temperature

The flue gases mass flow and the adiabatic flame temperature were already determined by the combustion model. Boiler geometry and walls characteristics were given by Ventil [13]. It was also assumed an average temperature for the surface walls set at 353.15 K.

The output data given by the heat transfer model is:

- Outlet flue gas temperatures at each boiler section
- Released energy in each slice of the furnace
- Released overall energy in the two convection sections

The schematic showed below sums up the entire process of energy transfer that occurs in each control volumes. The main focus of this project is to determine the amount of energy released in each control volume by the flue gases to the boiler internal surfaces.

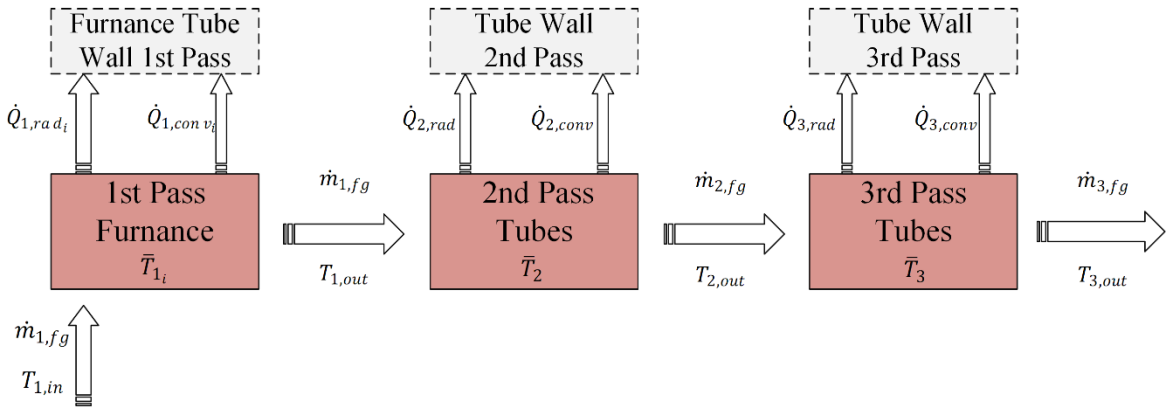

Figure 4.1. Proposed heat transfer modelling scheme.

4.2. Radiation Section

The combustion chamber is a vertical cylinder where heat is released by the flue gases to the surrounding walls and which are produced from the combustion of fuel with atmospheric air in the burner section (i.e., the combustion chamber's lower sector). From the papers studied, the furnace is also called radiation section because the amount of heat released occurs mainly due to radiation as observed by some experimental tests [13] [19]. Additionally, some case studies [20-21] stated that the transmitted energy by convection contributes, on average, to less than 20% of the total transferred energy. Using biomass as fuel may increase the radiation contribution even more since great amount of ashes and soot are produced during combustion, however, it will not be assumed in this work.

To model the radiation section the following assumptions were considered:

- Stationary conditions (constant mass flow)
- Complete combustion of the reactants
- Combustion chamber and inner tube surface are gray surfaces
- Excess air is constant

4.2.1. Fractional Heat Release

Translating the amount of energy transferred into a numerical model is very complex [22] since the released heat behavior from the flue gases is highly non-linear and the unpredictable turbulent flow containing soot and ashes around the internal section add further intricacy to the whole process.

The furnace's height has been discretized into N_i equal segments (i.e., slices) in order to determine the amount of energy transferred in each slice to the surrounding surfaces with greater exactitude. An energy balance considering the generated and released energy was established for each slice, as seen on the equation 4.1.

$$\dot{Q}_{1,in_i} - \dot{Q}_{1,out_i} = \dot{Q}_{1,conv_i} + \dot{Q}_{1,rad_i} \tag{4.1}$$

On the left side of the Equation 4.1, both the amount of energy that enters and exist each control volume may be calculated by the following equation:

$$\dot{Q}_{1,in_i} - \dot{Q}_{1,out_i} = \left(H_{1,in_i} - H_{1,out_i}\right) \tag{4.2}$$

Flue gases average properties such as emissivity, absorptivity, specific mass, dynamic viscosity, specific mass, heat capacity, Prandtl number and thermal conductivity were correlated with gas products' film temperatures and partial pressures mean values present in each slice, using Refprop database to gather the thermal properties of the combustion products.

The H_{1,in_i} and H_{1,out_i} are the products enthalpies in each segment and can be determined through the Refprop data as well as NASA's tables (See Annex A). The $\dot{m}_{1,fg}$ value is constant throughout the whole furnace section.

The heat transferred by convection to the surrounding inner walls in each segment, can be translated into:

$$\dot{Q}_{1,conv_i} = h_{1,conv_i} \frac{A_1}{N_i} \left(\bar{T}_{1_i} - \bar{T}_{wall}\right) \tag{4.3}$$

The convective coefficient is given by the following equation:

$$h_{1,conv_i} = Nu_{D,1}\left(\frac{\bar{k}_{1_i}}{D_{1,int}}\right)K_c \tag{4.4}$$

K_c is a convective calibration factor used to improve the convective heat coefficient values since the equations used for plains tubes do not work properly on this boiler's furnace section as the diameter measures almost the same as the section length [24]. After many simulations (see Annex C) pursuing an optimal value that would adapt to various boilers with different output power values, which were taken from the experimental data, it was proved that $K_c = 5$ was in good agreement with the all experimental output power parameters.

This factor took into account the convection average percentage demonstrated in study [13] and the overall compatibility within other various output thermal power values (see Annex C), showing acceptable results as proved in chapter 5. The parameter $\bar{k}_{1_i}$ is the mean flue gas thermal conductivity in each discretized slice.

The Nusselt number is defined by McAdam's correlations for turbulent mass flow rate and used solely for plain tubes, admitted by [15], [16] and [23]:

$$Nu_{D,1} = 0{,}023 Re^{0,8} Pr^{0,3} \tag{4.5}$$

Reynold's number depends on the internal furnace diameter, the mass flow value that was already determined by the previous combustion model and the flue gases dynamic viscosity which is evaluated by RefProp database where both film temperature (mean temperature between the mean flue gases and wall temperatures) and products partial pressures serve as input data to gather the mean viscosity value.

$$Re_{1_i} = \frac{4\,\dot{m}_{1,fg}}{\pi\, D_{1,int}\, \mu_{1,fg}} \tag{4.6}$$

Prandtl number can also be evaluated in MATLAB by the Refprop's data base. For gases, the Prandtl number varies insignificantly with the temperature with its values ranging between $0{,}70 < Pr < 0{,}75$.

The radiation zone geometry is difficult to measure due to its spherical top vessel and two irregular shape ducts. To minimize this geometry complexity, an equiavalent surface area of the furnace section was assumed, considering not only the furnace surface's area, but also the vessel and smoke ducts areas and half area of the 1st inversion box. Additionally, to reduce and simplify the calculations of all areas of this section, an equivalent length was considered while maintaining the furnace's internal diameter (1 m) as reference. This total area was estimated by the given dimensions of each boiler components supplied by Ventil [18], as also seen in Annex B. A schematic representation of an equivalent area for the 1st boiler pass is shown in Figure 4.2, while is calculation is showed in equation 4.7.

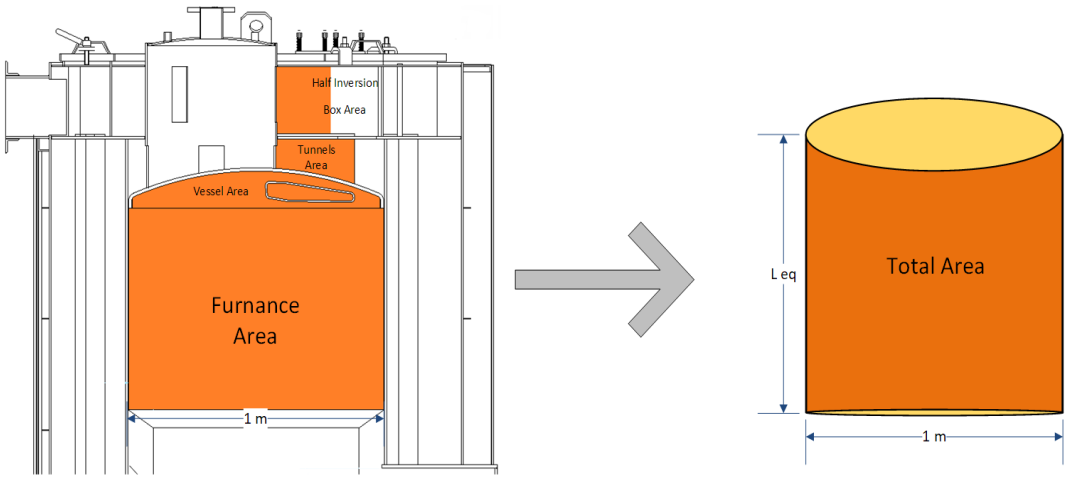

Figure 4.2. Calculation of the equivalent length and total volume of the furnace by simplifying the radiation section of the boiler biomass.

$$A_1 = A_{fur} + A_{vessel} + A_{ducts} + 0.5 * A_{InvBox_1} = \pi\, D_{1,int}\, L_{eq_{fur}} \tag{4.7}$$

The temperature in each slice is defined as the mean temperature between both starting temperature and the exit temperature of each single segment. This assumption is supported by studies [13] [17] and is expressed by:

$$\bar{T}_{1_i} = 0.5 * \left(T_{1_i,in} + T_{1_i,out}\right) \tag{4.8}$$

The inlet flue gases temperature of the first discretized slice equals to the adiabatic flame temperature, $T_{flame} = T_{1,in}$. Wall temperature is much lower than the gas temperature, given the minor amount of radiative heat released from the wall surface to the hot gases compared to the opposite direction [24]. It was assumed an average wall temperature value throughout the entire boiler surfaces (i.e., radiation and convection sections). This representative temperature is a sensible approach to predict the amount of released energy within the furnace when compared to experimental results.

Energy release by radiation to the inner walls is given by:

$$\dot{Q}_{1,rad_i} = A_1\, \sigma \left(\varepsilon_{1,_i} \bar{T}_{1_i}^4 - \alpha_{1_i} \bar{T}_{wall}^4\right) \tag{4.9}$$

$\bar{T}_{1_i}^4$ corresponds to the mean temperature of the combustion gases in each segment while $\bar{T}_{wall}^4$ is defined as a constant temperature along the furnace wall. A_1 corresponds to the whole irradiated section area i.e., the radiation heat in each slice is emitted to the whole furnace internal area. In addition, σ is the Boltzmann constant.

Under the assumption of gray gases and gray walls, Hottel and Sarofim [25-26] developed several procedures to calculate gaseous emission and absorption, stating that the radiative emissions are determined by the mean gas temperature of each slice.

To determine the emissivity from the Figures 4.3 (a) and (b), it is necessary to determine the radius L [24] of a gas which radiates to an element of area at the center of its base. This dimension has been replaced to a mean beam length L_e, which assumes the use of various gas geometries. The L_e was established to correlate the gas emissivity dependency on the size and shape of the flue gas geometry. In this work, the flue gases geometry is very irregular, so an arbitrary volume shape that radiates the whole surface area was considered and L_e was determine by:

$$L_e = \frac{3.6\, V_{i,slice}}{A_{1,int}} \tag{4.10}$$

$V_{i,slice}$ corresponds to the volume of one slice, while A is the total internal area of the furnace, since that volume segment radiates to the whole furnace area. The total gas emissivity ε_{fg} may be evaluated from the gas's temperatures and total pressure correlations, but also by the partial pressure of the radiative species (H_2O and CO_2) and the furnace dimensions.

The emitted heat by diatoms molecules can be ignored since the radiation emitted by triatomic molecules such as H_2O and CO_2 have much greater magnitude [21]. This assumption induces insignificant errors to the following calculations, thus, the total gas emissivity in each slice can be described as:

$$\varepsilon_{1,i} = \varepsilon_{H_2O} + \varepsilon_{CO_2} - \Delta\varepsilon \tag{4.11}$$

Where the radiative species H_2O and CO_2 are estimated by the upcoming figure:

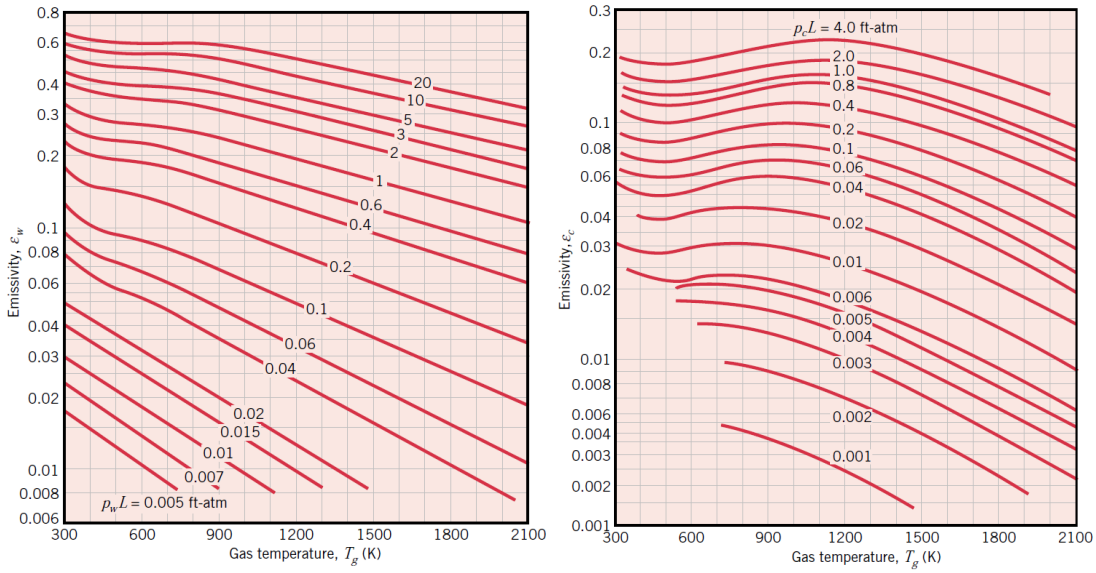

Figure 4.3. Emissivity of water (left) and carbon dioxide (right) in a mixture without radiating gases at 1-atm total pressure and considering hemispherical shape.

This calculation is applied when water vapor and carbon dioxide are separated in the gas mixture with other non-radiating species, nevertheless these results can be used for cases in which water vapor and carbon dioxide are mixed in the gas mixture. The correction factor $\Delta\varepsilon$ is defined as a reduction of the radiative emissivity associated with the radiation absorptivity between the radiative species and it is determined from Figure 4.4 for various gas temperatures.

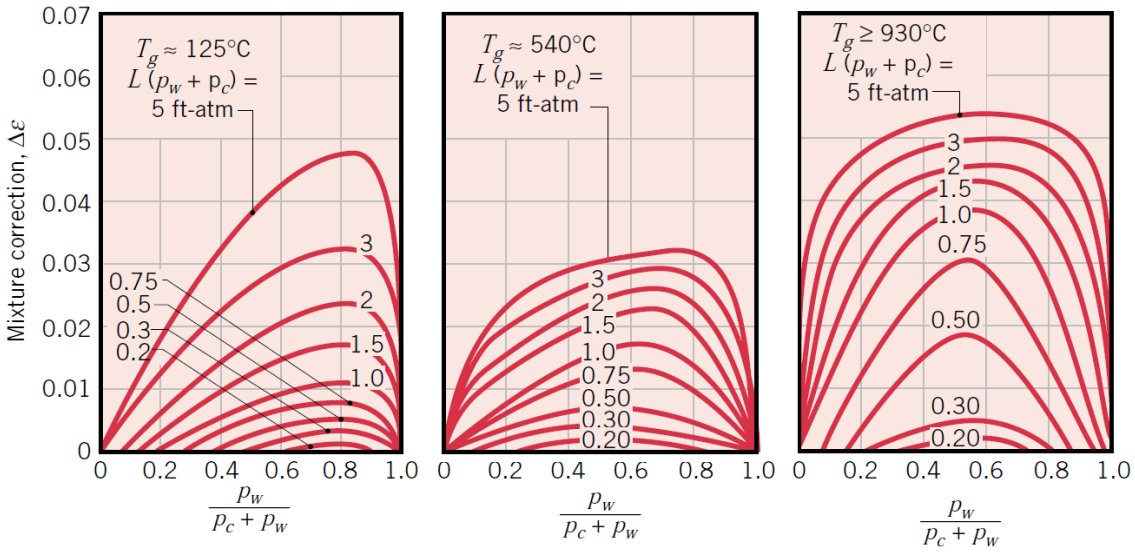

Figure 4.4. Corrective factor related to the mixtures of water vapor and carbon dioxide.

Gas absorptivity can be calculated from the gas's emissivity equations and from correlations demonstrated in [24], translating into this equation:

$$\alpha_{1,i} = \alpha_{H_2O} + \alpha_{CO_2} - \Delta\alpha \tag{4.12}$$

4.2.2. Mean Temperature Method

Several studied papers [13] [17] [23] showed that a developed model to predict the amount of heat transferred in a 3-pass fire-tube boiler can be done according to a bi-dimensional assumption, on both furnace and tube pass sections using, to evaluate the amount of energy transferred, an average temperature for each main boiler section. The two-axis of this bi-dimensional approach are defined as width (internal diameter) and length (or height) of each main sector. The length also corresponds to the furnace L_{eq}. This method uses both in and out-temperatures of the boiler main sections to determine the mean temperatures values. As the furnace was discretized in slices because of the complex heat flow behavior, no such approach was needed for the convection sections since they have simple cylinder forms which translates into straightforward correlations, producing also good results with minor discrepancies.

4.3. Convection Sections

After evaluating the amount of energy transferred in the radiation section, it is necessary to model the remaining boiler sections. To analyze the heat exchange inside the tubes pass, it was assumed some simplifications:

- The inversion boxes areas were converted into added equivalent smoke-tube areas.
- The mean temperature in the smoke tubes is constant.
- The flow rate is divided by the number of tubes in each section.

4.3.1. 1st Convection Section

The geometric dimensions considered in the 2nd pass include the whole 22 tubes area and two half areas of both first and second inversion box surfaces, as shown in the Figure 15. The total equivalent area of this section is determined by equation 4.13.

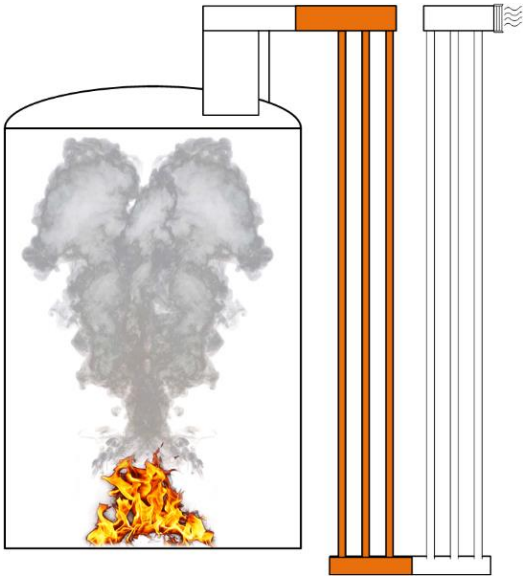

Figure 4.5. Total area of the 2nd pass represented in orange, which considers the area of the two sets of smoke tubes, and half of each inversion box.

$$A_2 = N_{1,tubes}\, A_{tubes} + 2 * \left(\frac{A_{InvBox}}{2}\right) = \pi\, D_{2,m}\, N_{2,tubes}\, L_{eq_{fur}} \tag{4.13}$$

The energy balance representing the heat exchanges in this section is adapted from [13] [23], and is expressed by:

$$\dot{Q}_{1,out} - \dot{Q}_{2,out} = \dot{Q}_{2,rad} + \dot{Q}_{2,conv} \tag{4.14}$$

The entering and exiting heat transmitted on the 1st convection section may be calculated through:

$$\dot{Q}_{1,out} - \dot{Q}_{2,out} = \dot{m}_{2,fg}\ \left(H_{2,in} - H_{2,out}\right) \tag{4.15}$$

Where:

$$\dot{m}_{2,fg}\ = \frac{\dot{m}_{1,fg}}{N_{2,tubes}} \tag{4.16}$$

Gas mass flow rate $\dot{m}_{fg,2}$ on the 2nd boiler pass is divided by the number of tubes, while the gas enthalpy values are evaluated from the Refprop database as mentioned on the radiation section.

In this section, the amount of radiative energy is lower than before due to the lower gas temperature. Radiation energy value is expected to be lower than the convective heat exchange because the radiative energy increases as the temperature of the flue gases increase as well (flue gases temperature elevated to the power of 4), therefore, as in this second pass, the average temperature of the gases is much lower than the combustion chamber.

$$\dot{Q}_{rad(fg,1-wall,1)} = A_{2,m}\ \sigma\ (\varepsilon_2 \bar{T}_2^4 - \alpha_2 \bar{T}_{wall}^4) \tag{4.17}$$

Emissivity and absorptivity depend on the section average temperature, therefore the values of ε_{fg} and α_{fg} are average for the whole sector. The $A_{2,total}$ is evaluated by the mean equivalent area of each tube and its $L_{eq,2}$ and multiplied by the number of tubes. $\bar{T}_{wall,2}$ is considered as the same temperature as $\bar{T}_{wall,fur}$.

The exchanged heat from the flue gases to the enveloped smoke tube walls is done mainly through convection, and which can be translated into:

$$\dot{Q}_{2,conv} = h_{2,conv}\, A_{2,m}\, (\bar{T}_2 - \bar{T}_{wall}) \tag{4.18}$$

Where:

$$\bar{T}_2 = \frac{T_{1,out} + T_{2,out}}{2} \tag{4.19}$$

The average temperature $\bar{T}_2$ of the flue gases is assumed to be uniform throughout the tubes length and results from the average temperature between the outlet of the furnace and the exit temperature at the 1st pass tubes.

The convection coefficient is used in thermodynamic models to determine the heat transferred occurred by convection effects. As seen from the radiation section the convective coefficient may be evaluated from McAdam's correlation [24], but it can be also expressed as:

$$h_{2,conv} = Nu_2 \frac{\bar{k}_{2,fg}}{D_{2,m}} \tag{4.20}$$

$\bar{k}_{2,fg}$ is the mean thermal gas conductivity and can be determined by the mass fraction and thermal conductivity k_i of each product substances. Using Refprop's database required two different data inputs, as for example, the mean temperature of the flue gases and each product substances' partial pressure to determine each k_i, then the overall thermal gas conductivity k_{fg} could be calculated by the follow expression:

$$\bar{k}_{2,fg} = k_{CO_2}\, f_{mass,CO_2} + k_{H_2O}\, f_{mass,H_2O} + k_{N_2}\, f_{mass,N_2} + k_{O_2}\, f_{mass,O_2} \tag{4.21}$$

The Nusselt number can also be described by other expressions cited by [13]. Idealized by Gnielinski [24], the use of this following equation is justified by the added

accuracy given to the Nusselt number for turbulent flow which equation also contains a corrective factor that takes into account the tubes D/L ratio [13].

$$Nu_{D,2} = \frac{\left(\frac{f_{2,fg}}{8}\right)(Re - 1000)\,Pr}{1 + 12{,}7\sqrt{\frac{f_{2,fg}}{8}}\left(Pr_2^{\frac{2}{3}} - 1\right)}\left[1 + \left(\frac{D_{2,m}}{L_{2,eq}}\right)^{\frac{2}{3}}\right] \tag{4.22}$$

Friction coefficient value is determined by the next equation for plain tubes [24].

$$f_{2,fg} = -1{,}8\log\left[\frac{6{,}9}{Re_2} + \left(\frac{\varepsilon_{r_2}}{3{,}7}\right)^{1{,}11}\right] \tag{4.23}$$

Where ε_r is the metal relative rugosity used on the inner walls, while ε_{abs} is the absolute rugosity which value is given by Ventil [13].

$$\varepsilon_{r_2} = \frac{\varepsilon_{abs}}{D_{2,m}} \tag{4.24}$$

To evaluate the Reynold number of one tube, the mass flow rate is divided by the number of 2nd pass tubes (i.e., $N_{2,tubes} = 22$) and the flue gas' dynamic viscosity is determined by the section mean temperature.

$$Re_2 = \frac{4\,\dot{m}_{2,fg}}{\pi\,D_{2,m}\,\mu_{2,fg}\,N_{2,tubes}} \tag{4.25}$$

4.3.2. 2nd Convection Section

The 2nd convection section total area include a set of 20 tubes, the half of the first inversion box and the entire second inversion box areas, as shown in the Figure 4.6.

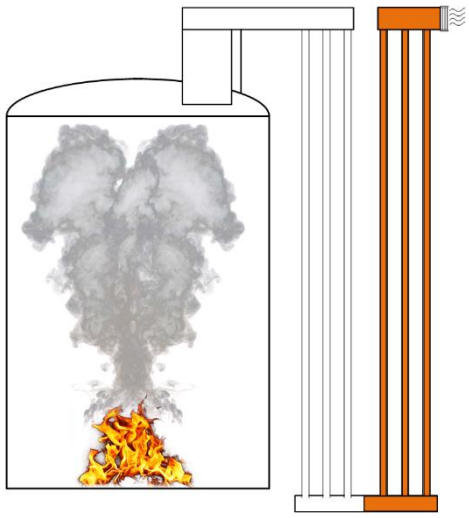

Figure 4.6. Total area of the 3rd pass represented in orange, which considers the area of the two sets of smoke tubes, half of the second inversion box and the whole third inversion box (chimney).

The A_3 is evaluated by the mean equivalent area of each tube, an equivalent length $L_{eq,3}$ and multiplied by the number of tubes. The overall section area is expressed by the following equation:

$$A_3 = N_{3,tubes}\, A_{tube} + \left(\frac{A_{InvBox}}{2}\right) + A_{chimney} = \pi\, D_{3,m}\, N_{3,tubes}\, L_{eq_3} \tag{4.26}$$

On this system's third pass, the flue gases release much less energy to the smoke tube surfaces because of the gas temperature decrease. The amount of energy carried by the gases tends to diminish proportionally as well. Based on studies [24-25] [29], radiating species have much less importance in this section due to that low gas temperatures, some studied papers even consider the radiation portion negligible. Nonetheless, the small amount of heat released by radiation was considered in this work.

Thermal balance which represents the total energy exchanged in the 2nd convection section, is displayed as:

$$\dot{Q}_{2,out} - \dot{Q}_{3,out} = \dot{Q}_{3,rad} + \dot{Q}_{3,conv} \tag{4.27}$$

The left side of the equation above can be translated into:

$$\dot{Q}_{2,out} - \dot{Q}_{3,out} = \dot{m}_{3,fg}\ \left(H_{3,in} - H_{3,out}\right) \tag{4.28}$$

Where:

$$\dot{m}_{3,fg}\ = \frac{\dot{m}_{1,fg}}{N_{3,tubes}} \tag{4.29}$$

Gast mass flow rate $\dot{m}_{3,fg}$ on the 3rd boiler pass is divided by the number of tubes, while the gas enthalpy values are evaluated from the Refprop data as mentioned on the radiation section.

$$\dot{Q}_{3,rad} = A_3\ \sigma\ (\varepsilon_3 \bar{T}_3^4 - \alpha_3 \bar{T}_{wall}^4) \tag{4.30}$$

Emissivity and absorptivity depend again, on the section average temperature, consequently, the values of ε_{fg} and α_{fg} are average for this entire section. Also, $\bar{T}_{wall,3}$ is considered as the same temperature as $\bar{T}_{wall,fur}$.

$$\bar{T}_3 = \frac{T_{2,out} + T_{3,out}}{2} \tag{4.31}$$

Where $T_{fg,3,out}$ is the exit temperature on the chimney and which was obtained by experimental results and used as initial input data on the previous combustion model. $T_{fg,2,out}$ is the starting temperature at the half of the second inversion box.

Along the boiler sections, the amount of heat released by the hot gases decreases gradually till the chimney where they are subsequently exhausted to the atmosphere. During the heat transfer process in this section, the convection fraction increases while the radiation diminishes even more compared to the 1st convection section due to the lower flue gas temperatures, thus convection has greater importance in this section (see also chapter 5).

Through the following equation, convective energy can be expressed as:

$$\dot{Q}_{conv(fg,2\rightarrow wall,2)} = h_{conv,2}\, A_3 \left(\bar{T}_{fg} - \bar{T}_{wall}\right)_3 \tag{4.32}$$

Convective heat transfer coefficient can be evaluated by the same equations as the 1st convection section i.e., expressions from 4.18 to 4.25. The average temperature values and the total area of this section were already determined as well, so the heat transferred by convection can be calculated for the 3rd boiler pass.

4.4. Model Calculation Process

To evaluate the overall boiler output power, a comprehensive model process is represented in the following chart (Figure 4.7).

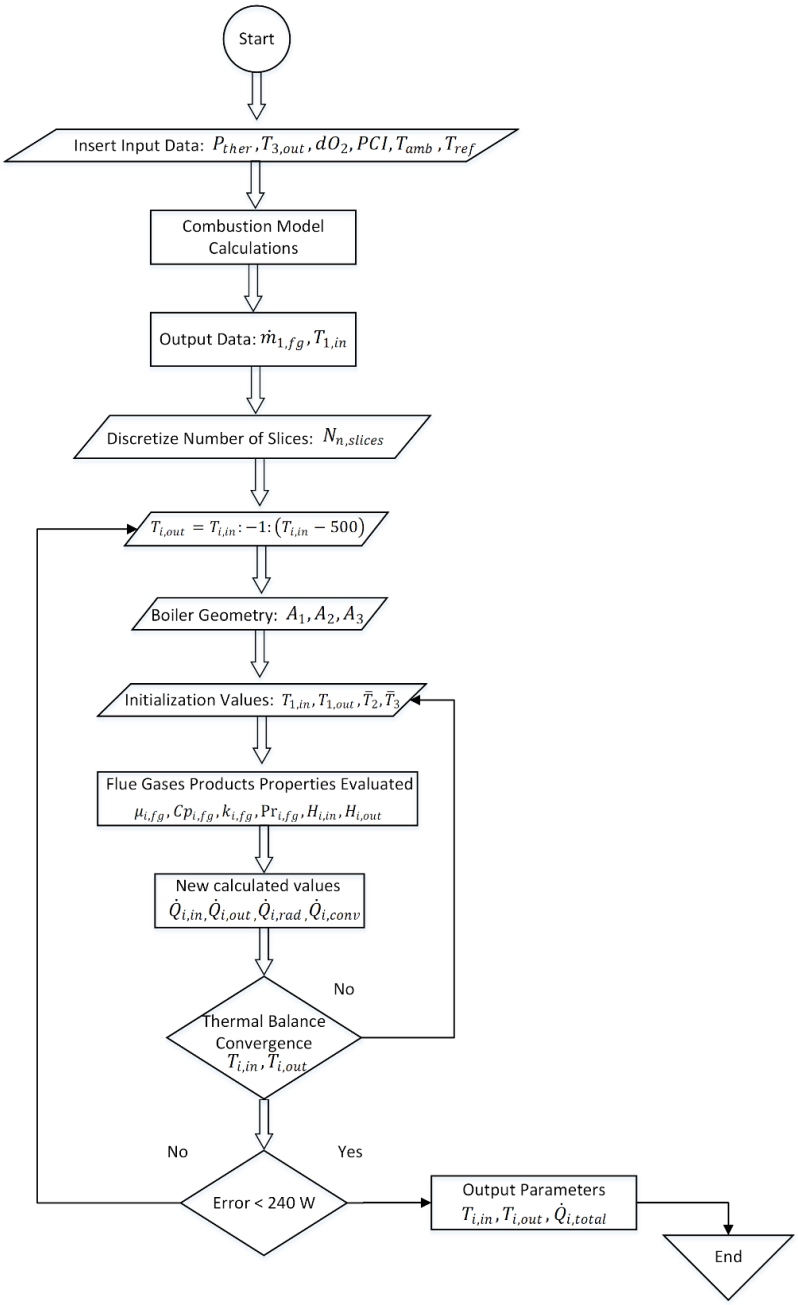

Figure 4.7. Process calculation by the heat transfer model to determine output parameters.

5. DATA ANALYSIS

5.1. Combustion Model

After an explicit explanation of the combustion model in chapter 3, some parameters such as the excess air O_2 (in products), ambient and biomass moistures were altered to comprehend which input data has greater influence on the adiabatic flame temperature and on the flue gas mass flow rate.

To this extent, the value of excess air was changed while the remaining initial data inputs were retained.

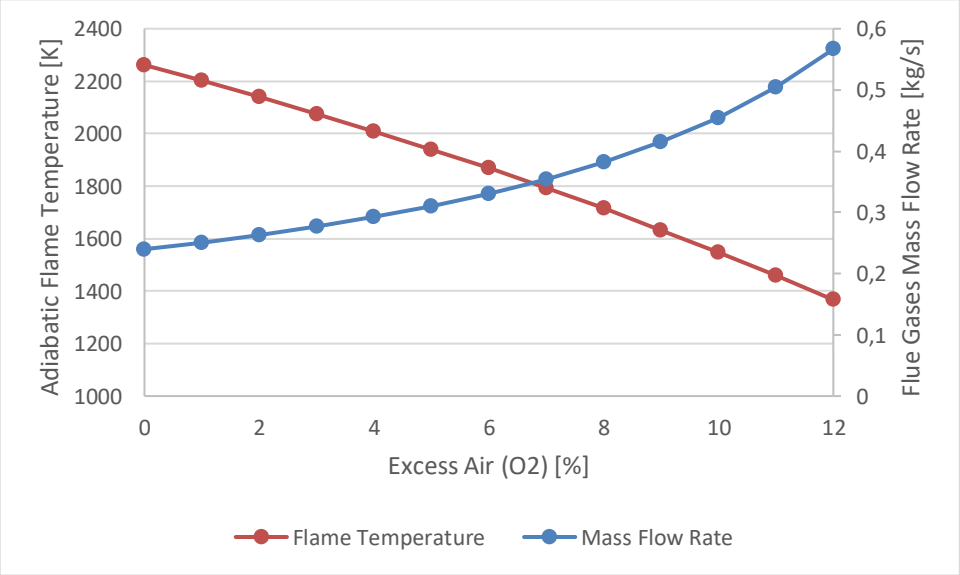

Figure 5.1. Flame temperature and flue gases mass flow value by changing the quantity of excess air in the products side.

From Figure 5.1, it is shown that the increasing the products excess air will linearly decrease the flame temperature considerably since too much air quantity will not be consumed by the flames and thus, will affect the combustion process. However, the flue gases mass flow rate will benefit exponentially when increasing excess air due to the additional air introduced that will flow throughout the boiler sections.

For different values of the boiler's thermal output power, the mass flow rate changes proportionally, as seen by the Figure 5.2.

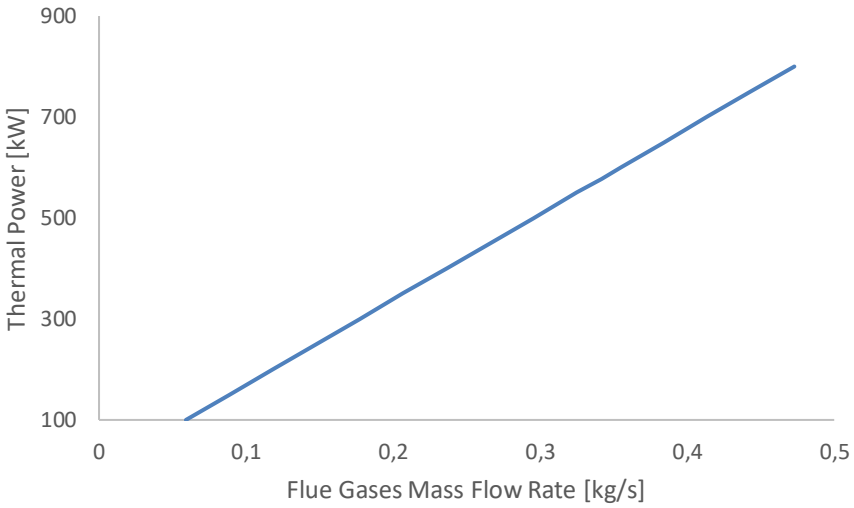

Figure 5.2. Flue gases mass flow increases proportionally with the boiler's output power.

The presence of moisture in both ambient air and biomass will also negatively influence the adiabatic flame temperature. To test the adiabatic flame temperature changes, moisture quantities were altered while maintaining the other input data as previous reference values. Below, the Figure 20 shows that increasing the amount of biomass' moisture will greatly decline the flame temperature value. This linear behaviour is explained by the vaporization process, i.e., the added energy needed to vaporize the liquid water present on the biomass (consuming energy).

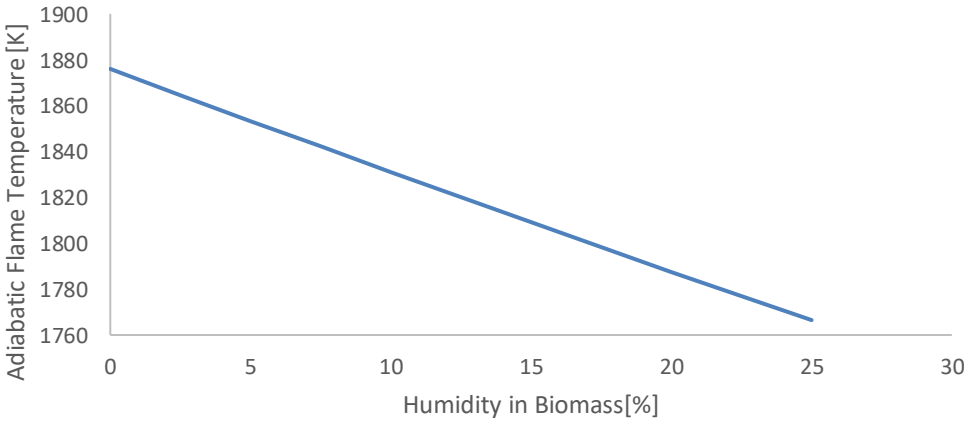

Figure 5.3. Influence of biomass moisture on the adiabatic flame temperature.

Increasing the amount of moisture present in ambient air (gaseous state) as seen in the following Figure 5.4, slightly affects the flame temperature value since the water molecules require more energy than air molecules to reach a determined temperature, i.e., the water has a higher specific heat value than the ambient air.

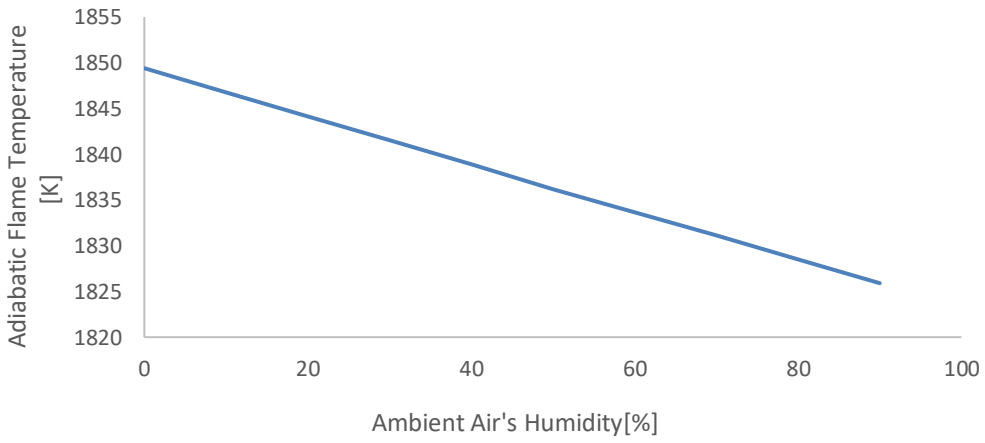

Figure 5.4. Influence of ambient air moisture on adiabatic flame temperature.

5.2. Heat Transfer Model

This study aims to provide a heat transfer model based on this 3-pass fire-tube boiler. In order to translate the heat exchange numerically, the taken approaches were based on various thermodynamic correlations and equations as mentioned in the chapter 4. Hence, various temperature results and released energy were determined in every boiler section by this model. With this amount of data collected by this heat transfer model, it is possible to evaluate its accuracy trough comparisons with experimental obtained data from real tests. Parameters such as power output, outlet furnace temperature and chimney temperature were evaluated by the model and compared against real value to validate the data and measure the error differences.

5.2.1. Radiation Section

The furnace section is where a large amount of energy is released. Thus, slices method was adopted to see in detail how much energy in form of radiation and convection is released in each slice and to better understand its behaviour on the radiation zone.

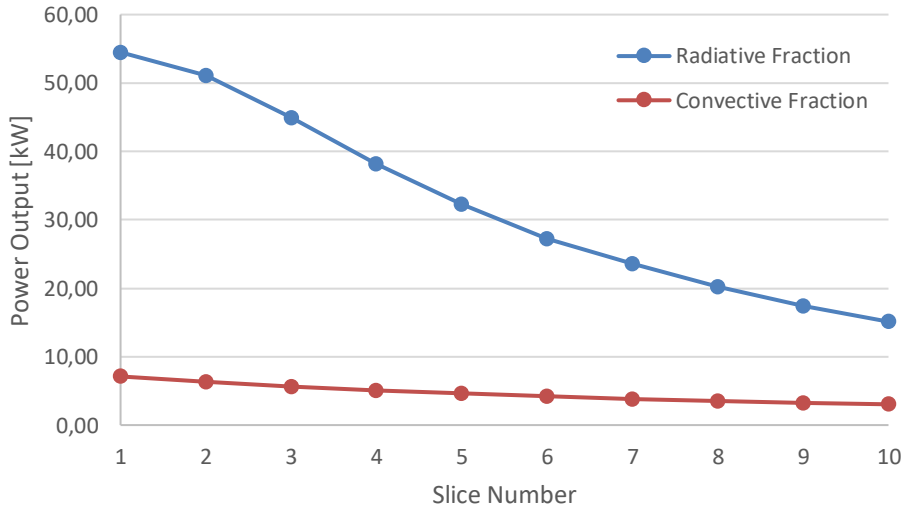

Figure 5.5. Power released by radiation and convection in each discretized slice.

Figure 5.5 shows the correlation between the maximum amount of radiative energy released on the first slices due to the higher temperatures. As the flue gases ascend, the temperature falls gradually in each slice promoting a decrease of the radiative fraction.

	Radiation Power [kW]	Convection Power [kW]	Total Power [kW]	Average Radiative Fraction [%]
Total [kW]	324,52	46,66	371,18	87,43

Figure 5.6. Power released by radiation and convection in the furnace.

As mentioned before, the heat transfer within the 1st boiler pass is mainly due to radiation with 87,47% of the total amount of energy released. The 324,52-kW output power released by radiative emissions make up 56% of the whole boiler power. Experimental data gathered from six different boiler operations were used. The values of each output power, excess air (products), outlet furnace and chimney temperatures were then compared against the heat transfer model calculations.

Output Power [kW]	Furnace Outlet Temperature [K]	Products Excess Air [%]	Chimney Temperature [K]
259,31	841,78	7,20	422,78
322,38	898,65	7,60	443,65
460,38	983,90	8,30	486,90
507,99	1012,30	7,40	491,30
578,00	1050,10	6,50	500,10
629,23	1073,50	5,90	505,51

Figure 5.7. Output power values and outlet temperatures obtained by six experimental boiler tests.

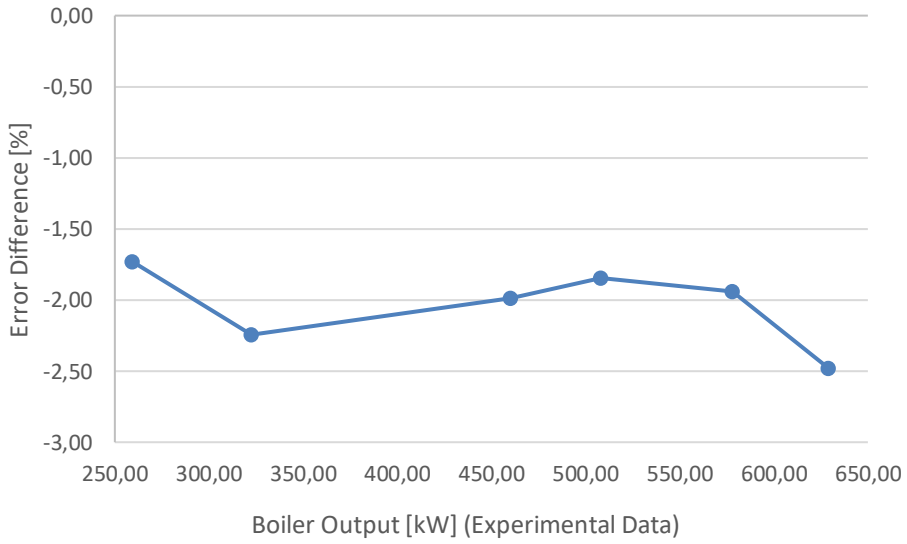

Figure 5.8. Heat Transfer Model error difference for various output power experimentally obtain.

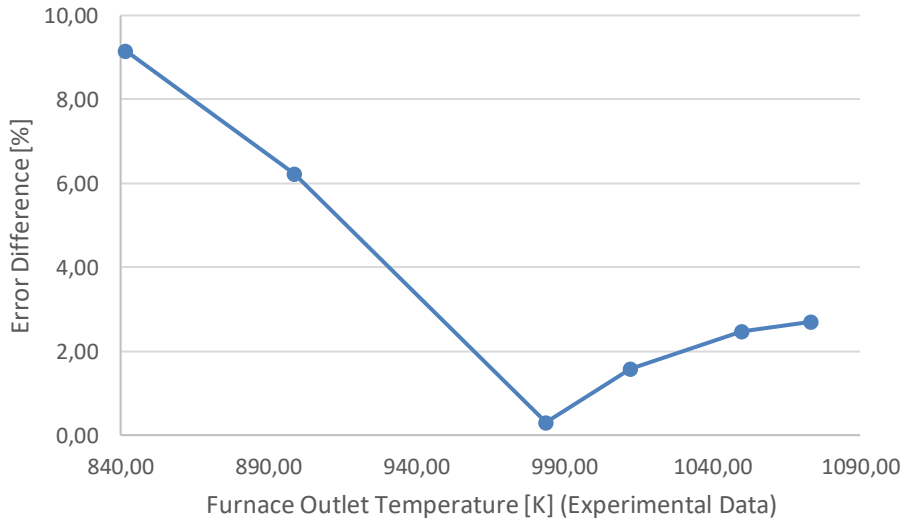

Figure 5.9. Model's outlet temperature error compared to experimental data.

As seen by the Figures 5.8 and 5.9 the heat transfer model produces acceptable results for the majority of the experimental tests. Note that, each blue dot in both figures represent the thermal power of each boiler tested.

The main error differences from these six boiler operations are explained by the furnace area simplifications where an equivalent length containing half area of the first inversion box was assumed as part of the furnace. This justifies on why the model furnace outlet temperatures were lower than the experimental obtained values. The first two error blue dots can be explained by the low boiler thermal power which this model was not aimed

to simulate and because of the less suitable value of the convective calibration factor admitted.

5.2.2. Convection Sections

In these sectors, as mentioned earlier, was applied a mean temperature method to obtain the heat released and outlet temperatures in each convection section. This technique showed good results since the used flow equations were based on plain tubes which worked well for these tubes while respecting the $L_{eq}/D > 60$ ratio [24]. The slice approach would offered greater discretization and better accuracy on heat release values. However, that would come at a cost of an increased longer computational time while the results would not diverge in great scale, providing negligible differences.

For initial conditions as referred in chapter 4, the power release analysis in these sections were calculated by the model for the 578-kW 3-pass smoke-tube boiler with 6,5% of excess air in the products.

	Radiation Power [kW]	Convection Power [kW]	Total Power [kW]	Convective Fraction [%]
Total [kW]	18,77	113,32	132,09	85,79

Figure 5.10. 1st Convection pass with radiative and convective heat quantities and overall convective fraction.

	Radiation Power [kW]	Convection Power [kW]	Total Power [kW]	Convective Fraction [%]
Total [kW]	6,08	57,67	63,75	90,46

Figure 5.11. 2nd Convection pass with radiative and convective heat quantities and overall convective fraction.

Power output in both convection section was obtained from the model data showed in Figures 5.10 and 5.11. The radiation heat release fraction is on average less than 15% in the 2nd boiler pass section and even less than 10% on the 3rd pass. This large gap is due to the average low temperatures in each convections section which do not promote great amount of radiative energy.

On the 2nd convection section the overall power release is less than 50% when compared to the former section as much of the energy was already transferred when flue gas temperatures were higher.

As the flue gases reach the chimney all the simplifications made till now are more pronounced and are reflected in the chimney temperature values, nonetheless the difference between the temperature values from the heat transfer model and the presumable ideal temperature results do not affect the great model' output power results which is the most important parameter.

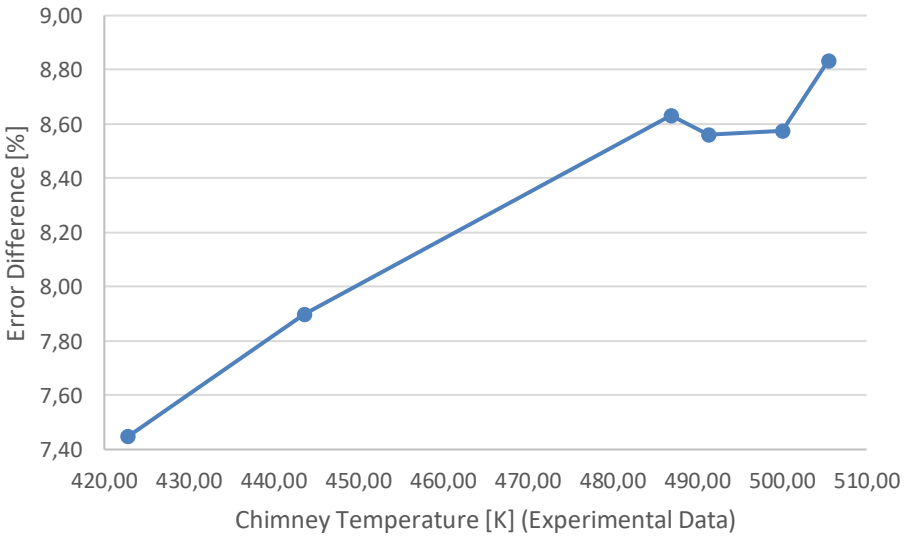

Figure 5.12. Model's chimney temperature error compared to experimental results.

5.3. Performance coefficient

In this study last analysis, it is interesting to see how much power is released along 3 main sections and how important the radiation section is. As proved by the output power results in each section (Figure 5.13), the radiation section produces the most energy (over 65%).

Boiler Sections	Total Power [kW]	Power Fraction [%]
Radiation Section	371,18	65,46
1st Convection Section	132,09	23,30
2nd Convection Section	63,75	11,24
Boiler Total Power [kW]	567,02	100

Figure 5.13. Power fractions of the three main boiler sections.

6. CONCLUSIONS

The demand of heat power domestic appliances using green alternative fuels have been increasing over the year. There is now a competitive market which forced the boilers price to reach a new low. Using bio fuels is also an advantage since it reduces the greenhouse gases to the atmosphere while being renewable by using forest waste. The biomass price per energy is also more attractive than natural gas or oil for domestic heat appliances.

To this extent, there is a need to develop and evaluate this type of boilers in order to make them even more efficient by understanding its heat transfer process. Thus, a complete heat transfer model has been developed from the ground up to numerically translate the energy transfer occurred in a 578-kW 3-pass fire-tube boiler. Hence, some experimental parameters from the studied boiler served has input data to start the combustion model.

These evaluated parameters provide various insights on the amount of radiative and convective energy transferred in each boiler section, demonstrating also, why the flame temperature and consequently, the heat radiation process are so important in the combustion chamber section and on the overall boiler output power.

Existing experimental data used in this work were limited and prevented better results within the model, hence, additional tests needed to be done to possibly recalibrate the convective calibration factor and improve the model. To further enhance the results, ashes and soot must be taking into account since their radiative emissions can be accountable as an additional energy transferred.

This model has high adaptability and can be used to evaluate heat transfer parameters for boilers with different geometries and power outputs. It can also simulate the amount surface area needed to produce a required power output.

Finally, this model may be used to design and develop new fire-tube boilers and might help various research projects since it easily adapts to different stationary operating conditions and for other types of fuel.

BIBLIOGRAPHY

[1] W. E. Council, "World Energy Resources Bioenergy," 2016. [Online]. Available: https://www.worldenergy.org/wp-content/uploads/2017/03/WEResources_Bioenergy_2016.pdf [Accessed: 06-Feb-2019].

[2] EIA, "Biofuels production drives growth in overall biomass energy use over past decade," *US Energy Information Administration*, 2014. [Online]. Available: https://www.eia.gov/todayinenergy/detail.php?id=15451 [Accessed: 06-Feb-2019].

[3] "Share of renewable energy in gross final energy consumption," 2017. [Online]. Available: https://www.eea.europa.eu/data-and-maps/indicators/renewable-gross-final-energy-consumption-4/assessment-2 [Accessed: 14-Oct-2018].

[4] "Energy database." [Online]. Available: https://ec.europa.eu/eurostat/en/web/energy/data/database [Accessed: 19-Jun-2018].

[5] Associação Portuguesa de Energias Renováveis, "Março 100 % renovável - primeiro mês com consumo de eletricidade assegurado por fontes renováveis é record de enorme relevância," 2018. [Online]. Available: https://www.apren.pt/pt/marco-100-renovavel--primeiro-mes-com-consumo-de-eletricidade-assegurado-por-fontes-renovaveis-e-record-de-enorme-relevancia [Accessed: 18-Jun-2018].

[6] APE, Deloitte "A Energia em Portugal." [Online]. Available: http://www.apenergia.pt/uploads/docs/Estudo_A_Energia_em_Portugal.pdf [Accessed: 20-Nov-2018].

[7] EIA, "Renewable Energy Consumption: Industrial and Transportation Sectors," 2019. [Online]. Available: https://www.eia.gov/totalenergy/data/monthly/pdf/sec10_5.pdf [Accessed: 06-Feb-2019].

[8] "State of play on the sustainability of solid and gaseous biomass used for electricity, heating and cooling in the EU," 2014. [Online]. Available: https://ec.europa.eu/energy/sites/ener/files/2014_biomass_state_of_play_.pdf [Accessed: 19-Jun-2018].

[9] A. Sá da Costa, "Eletricidade Renovável no Contexto Atual," 2015. [Online]. Available: http://www.ordemengenheiros.pt/fotos/dossier_artigo/apren_oeng_debate_18_06_2015_final_1071437210558bd767900c0.pdf [Accessed: 14-Jun-2018].

[10] EIA, "Renewable Energy Production and Consumption by Source," 2019. [Online]. Available: https://www.eia.gov/totalenergy/data/monthly/pdf/sec10_3.pdf [Accessed: 06-Feb-2019].

[11] EIA, "Renewable Energy Consumption: Residential and Commercial Sectors," 2019. [Online]. Available: https://www.eia.gov/totalenergy/data/monthly/pdf/sec10_4.pdf [Accessed: 06-Feb-2019].

[12] D. Drysdale, *An introduction to Fire Dynamics*, Second Edi. Chichester, England: John Wiley & Sons, 1999.

[13] A. Abene, A. Rahmani, R. G. Seddiki, A. Moroncini, and R. Guillaume, "Heat Transfer Study in 3-Pass Fire-Tube Boiler During a," vol. i, no. 4, pp. 57–64, 2017.

[14] Y. A. Çengel and M. A. Boles, *Thermodynamics: An Engineering Approach*, 8th ed. McGraw-Hill, 2014.

[15] A. Rahmani, "Numerical Investigation of Heat Transfer in 4-Pass Fire-Tube Boiler," *Am. J. Chem. Eng.*, vol. 2, no. 5, p. 65, 2014.

[16] F. J. Gutiérrez Ortiz, "Modeling of fire-tube boilers," *Appl. Therm. Eng.*, vol. 31, no. 16, pp. 3463–3478, 2011.

[17] A. Bisetto, D. Del Col, and M. Schievano, "Fire tube heat generators: Experimental analysis and modeling," *Appl. Therm. Eng.*, vol. 78, pp. 236–247, 2015.

[18] "Caldeiras Ventil CVT." [Online]. Available: http://ventil.pt/pt/produto_detalhes/2/55/caldeiras-ventil-cvt [Accessed: 14-Jun-2018].

[19] R. Siegel and J.R. Howell, *Thermal radiation heat transfer*. 6th Edition, CRC Press, New York. USA, 2015.

[20] M. Tamotsu, "Fire tube boiler," vol. 16, no. Applied Thermal Engineering, pp. 3–8, 1996.

[21] R. Borghi and M. Destriau, *La combustion et les flammes*. Edition Technip, Paris, 1995.

[22] B. Leckner, "Radiation from flames & gases in a cold-wall combustion chamber," *Heat Mass Transf.*, vol. 13, pp. 185–197, 1970.

[23] K. Sørensen, C. M. S. Karstensen, T. Condra, and N. Houbak, "Modelling and simulating fire tube boiler performance," *Water*.

[24] F. P. Incropera, D. P. DeWitt, T. L. Bergman, and A. S. Lavine, *Fundamentals of Heat and Mass Transfer*. 2007.

[25] H. H.C. and S. A.F., *Radiative Transfer*. New York, USA: McGraw-Hill, 1967.

[26] H. C. Hottel, *Radiant-Heat Transmission*, 3rd ed. New York, USA: McGraw-Hill, 1954.

ANNEX A

Molar fractions of each product substance in a real reaction were calculated from the chemical balance equations seen in Figure 26.

```
%%  Real reaction with 6.5% of excess air (O2) with 10% of moisture present in biomass and 70% of moisture present in the combustion air
% /Reference reaction to evaluate the output data of the combustion model/
% x_hum_t*(C H O N+n_H2O_bio)+L(O2+3.76N2)+n_amb_ar_reag)->a_hum_t*CO2+b_hum_t*H2O+c_hum_t*N2+d*O2

quanti_hum = L_hum*4.76;                                % Moisture quantity present in dry air as exemplified in Thermodynamics (Çengel et al) (Example 15-3, Page 767 and 768)
P_sat=refpropm('P','T',T_amb,'Q',0,'water');            % Saturated pressure at combustion air temperature and vapor fraction set to 0 (Q=0 --- Solely saturated water)
P_amb=H2O_amb_air*P_sat;                                  % Partial pressure of the combustion air moisture
n_H2O_hum_amb=(((P_amb/P_atm)*quanti_hum))/x_hum;         % Molar fraction of combustion air moisture in the reactants
n_H2O_hum_amb_2=((P_amb/P_atm)*(quanti_hum/x_hum))/(1-(P_amb/P_atm));   % Another purposed equation with similar results

x_hum_t=(2-7.52*d-2*d)/(n_N+7.52*a+3.76*b_hum_st-3.76*n_O-3.76*n_H2O_bio+2*a);% The b_hum_st portion do not inclue ambient moisture since its value do not change with x_hum_t
a_hum_t=a*x_hum_t;                                                              % Molar fraction of CO2
b_hum_t=(x_hum_t*((n_H/2)+n_H2O_bio))+(n_H2O_hum_amb*x_hum_t);                  % Molar fraction of H2O
L_hum_t=(2*a_hum_t+b_hum_t+2*d-n_O*x_hum_t-n_H2O_bio*x_hum_t-n_H2O_hum_amb*x_hum_t)*0.5; % Excess air
c_hum_t=(n_N*x_hum_t+7.52*L_hum_t)/2;                                           % Molar fraction of N2

n_CO2_real=a_hum_t/x_hum_t;                             % [kmol] Molar fractions of the products for 1kmol of dry biomass
n_H2O_real=b_hum_t/x_hum_t;
n_N2_real=c_hum_t/x_hum_t;
n_O2_real=d/x_hum_t;
n_t_real=n_CO2_real+n_H2O_real+n_N2_real+n_O2_real;     % Total number of moles in the products
```

Figure A.1. Chemical balance equations for a real reaction situation with moisture in both ambient air and biomass.

As mentioned in chapter 3.4.3, evaluating the adiabatic flame temperature was done by matching the reactants and flame enthalpy energies with a maximum admissible error of 50 kJ as shown in the next Figure 26.

```
T_flame=1000; %[K]- Start temperature
error=50;     %[kJ]- Error margin
while error>1
 %[kJ] - Enthalpies of each chemical compound
(products side) at flame temperature
H_Tflame_CO2=0.0056*T_flame^2+41.443*T_flame-406958;
H_Tflame_H2O=0.0058*T_flame^2+29.625*T_flame-251191;
H_Tflame_O2=0.0026*T_flame^2+29.025*T_flame-8855.9;
H_Tflame_N2=0.0023*T_flame^2+27.887*T_flame-8598.7;

%[kJ] - Flame total energy
E_flame=(n_CO2_real*hf_CO2)+(n_H2O_real*hf_H2O)+(n_CO2
_real*(H_Tflame_CO2-
H_Tref_CO2))+(n_H2O_real*(H_Tflame_H2O-
H_Tref_H2O))+(n_N2_real*(H_Tflame_N2-H_Tref_N2))+(n_O2
_real*(H_Tflame_O2-H_Tref_O2));%[kJ] - Flame energy

error=abs(E_reagents-E_flame);%[K]- Absolute error
value

if error>1
    T_flame=T_flame+error*0.001; %[K]- Output value of
the flame temperature

end
end %Loop ended
```

Figure A.2. Flame temperature evaluation using a “while” cycle on MATLAB

ANNEX B

The 2D boiler drawings provided by the boiler supplier Ventil are displayed below.

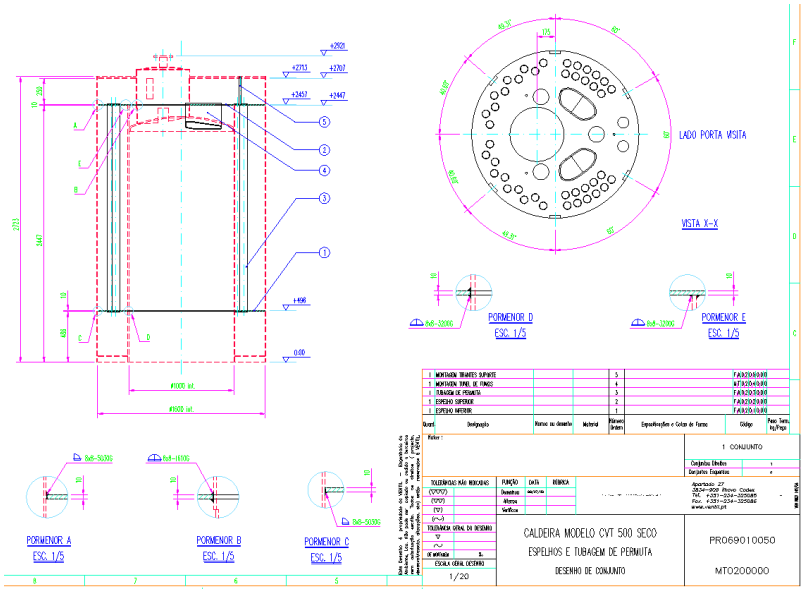

Figure B.1. Boiler dimensions with detailed tube geometries.

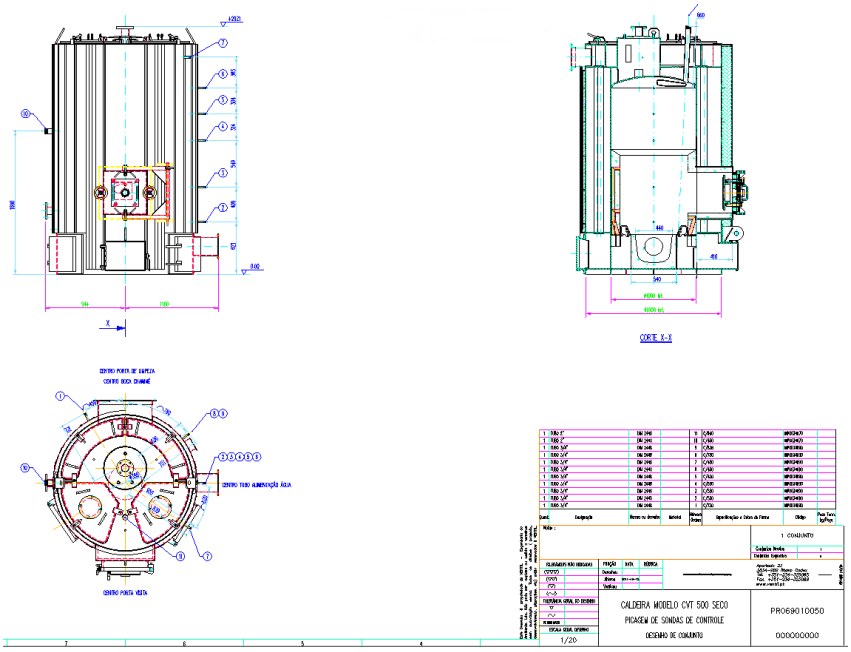

Figure B.2. Boiler top and side dimensions.

From Ventil's website, some parameters for the studied boiler can been examine through the following table.

CVT-SMODEL Modelo CVT-S | Modelo CVT-S		300	500	750	1.000	1.250	1.500	2.000	3.000	4.000	5.000	6.000
Nominal Power Output Potencia Térmica Nominal Potência Térmica Nominal	kW_{th}	350	580	870	1.160	1.450	1.750	2.320	3.480	4.640	5.800	7.000
	kcal/h	300.000	500.000	750.000	1.000.000	1.250.000	1.500.000	2.000.000	3.000.000	4.000.000	5.000.000	6.000.000
Dimension A (hieght) Dimensión A (altura) Dimensão A (altura)	mm	2.600	2.930	3.210	3.770	3.820	3.960	3.960	4.810	5.110	5.600	6.250
Dimension B (diameter) Dimensión B (diámetro) Dimensão B (diâmetro)	mm	1.430	2.050	2.100	2.320	2.400	2.440	2.580	3.110	3.400	3.700	4.160
Boiler House (minimum height) Altura mínima necesaria en la instalación Casa da caldeira (altura mínima)	m	4,5	5	5	5,5	5,5	6	6	7	8	8	9
Heat Transfer Area Superficie de transferencia térmica Área do permutador	m^2	16	24	35	52	65	79	86	174	230	314	362
Weight Peso Peso	kg	2.500	4.200	4.800	8.100	9.200	10.000	12.000	21.000	29.500	34.500	39.000
Water Capacity Volumen de agua Volume de água	dm^3	1.350	2.200	2.450	4.900	5.700	6.100	6.150	9.900	14.000	16.500	19.200
Maximum Water Temperature Temperatura máxima del agua Temperatura máxima da água	°C			109								
Average Thermal Efficiency Eficiencia Térmica Eficiência Térmica	%			85,9-89,8								
Maximum Fuel Consumption (pellets) Consumo máximo de combustible Consumo máximo de combustível	kg/h	83-87	138-144	207-216	276-288	346-360	417-434	554-577	832-866	1.108-1.154	1.380-1.440	1.670-1.735

Figure B.3. Boiler characteristics given by Ventil.

ANNEX C

Six different boilers, each with different output power values are displayed in the Figure 37, where furnace and chimney outlet temperatures were evaluated.

Experimental Data		
Overall Boiler Output Power [kW]	Furnace Outlet Temperature [K]	Chimney Temperature [K]
259,31	814,5	423,8
322,38	869,35	443,85
460,38	992,5	503,15
507,99	1021,1	509,9
578	1045,9	519,15
629,23	1055,1	515,85

Figure C.1. Data gathered by experimental tests using thermocouples to evaluate outlet temperatures.

As seen below, some boiler parameters were determined by the heat transfer model using several calibration factors. To select the optimal factor value to accurately match, in the best way possible, the experimental results. The lowest error difference on the boiler outlet power was the main parameter taken into account when choosing the calibration value. Although, the calibration factor value 10 would give the best results in terms of error differences, it did not work well for the 628-kW boiler test. Proving that this factor is not suitable for high powered boilers. Thus, the best calibration values were between 5 and 6, where the value 5 was chosen solely for its lower error difference of the overall boiler thermal power.

Heat Transfer Model Data							
Boiler	Furnace				Chimney	Boiler	Chimney
Calibration Factor = 1							
Overall Boiler Output Power [kW]	Furnace Total Power [kW]	Radiation Power [kW]	Convection Power [kW]	Furnace Outlet temperature [K]	Chimney temperature [K]	Power Difference [%]	Temperature Difference[%]
254,4	196,9	193,36	3,54	792,78	462,78	1,89348656	8,423008773
313,92	225,92	221,1	4,82	873,65	487,65	2,624232272	8,981851738
448	272,54	264,6	7,94	1021,9	541,9	2,689082931	7,150765824
494,9	301,28	292,7	8,58	1036,3	546,3	2,576822378	6,663005675
563,58	352,42	342,74	9,68	1068,1	557,05	2,494809689	6,803698052
609,63	381,88	371,45	10,43	1088,5	569,51	3,114918233	9,422134818
Calibration Factor = 3							
254,86	199,4	188,96	10,44	778,78	459,78	1,716092708	7,825481752
314,68	229,76	215,55	14,21	857,65	484,65	2,388485638	8,418446301
449,5	280,24	256,85	23,39	1000,9	537,91	2,363265129	6,462047554
496,75	316,67	291,4	25,27	1015,3	542,3	2,212641981	5,974552831
565,1	361,7	333,2	28,5	1046,1	552,1	2,23183391	5,968121717
548,2	392,14	361,44	30,7	1065,5	474,52	12,8776441	-8,709854168
Calibration Factor = 4							
254,7	200,2	186,4	13,8	771,8	458,78	1,777794917	7,62456951
314,9	231,38	212,6	18,78	849,65	483,65	2,320243191	8,229091285
450,3	284,3	253,4	30,9	989,9	535,9	2,189495634	6,111214779
497,5	320,8	287,4	33,4	1005,3	539,3	2,06500128	5,451511218
566,2	366,5	328,8	37,7	1035,1	550,1	2,041522491	5,626249773
611,2	396,7	356,2	40,5	1053,5	556,5	2,865406926	7,30458221
Calibration Factor = 5							
254,89	201,5	184,38	17,12	764,78	456,78	1,704523543	7,220105959
315,31	233,35	210,06	23,29	842,65	481,65	2,193064086	7,848022423
451,43	558,54	520,22	38,32	980,91	532,91	1,944046223	5,584432643
498,83	324,96	283,56	41,4	996,28	537,28	1,803185102	5,096039309
567,02	371,18	324,52	46,66	1024,10	547,05	1,899653979	5,100082259
613,95	402,33	352,05	50,28	1044,50	554,52	2,428364827	6,973598788
Calibration Factor = 6							
254,95	202,55	182,18	20,37	757,78	455,78	1,681385215	7,016543069
315,56	234,98	207,28	27,7	834,65	480,65	2,115515851	7,656298762
451,1	291,6	246,1	45,5	968,91	530,91	2,015726139	5,22875817
499,3	328,66	279,44	49,22	986,3	535,3	1,710663596	4,745002802
567,6	375,48	320	55,48	1013,1	545,05	1,799307958	4,751857628
613,88	406,81	347,05	59,76	1032,5	551,52	2,439489535	6,467580505
Calibration Factor = 10							
256,2	207,1	174,2	32,9	734,78	450,8	1,199336701	5,989352263
316,7	242,05	197,4	44,65	803,65	473,7	1,761895899	6,301456618
455,5	307	233,6	73,4	932,9	521,9	1,059993918	3,592642269
502,9	344,48	265,22	79,26	947,28	526,28	1,001988228	3,112411644
571,7	392,9	303,6	89,3	974	536	1,089965398	3,143656716
525,7	364,95	278,6	86,35	901,5	519,52	16,4534431	0,706421312

Figure C.2. Power and temperature values for various convective calibration factors. The calibration factor with the value 10 shows that the last thermal power (ideally 629,23 kW) value does not correspond to what was expected, so this factor was dismissed.